Environment, Development and Sustainability
https://doi.org/10.1007/s10668-023-04350-2

Techno-economic analysis of renewable energy sources' potential in the rural northern region of Kalam in Pakistan

Shayan Tariq Jan[1] · **Abdulaziz Alanazi**[2] · **Majid Feroz**[1] · **Mohana Alanazi**[3]

Received: 5 July 2023 / Accepted: 12 December 2023

Abstract
In the face of escalating global energy demands and the unpredictable nature of renewable resources, the quest for sustainable and reliable power solutions has never been more pressing. Hybrid power systems, which integrate multiple energy sources, have emerged as a beacon of hope, particularly for remote and rural regions with limited or no connection to the national power grid. This study provides an in-depth analysis to determine the optimal hybrid energy system, considering diesel, wind, solar, and hydro sources, for a local load of 20 kW in the rural area of Bankhwar Utrar in Kalam, Pakistan. The study considered the energy profile for an entire year while the research was conducted from September to December 2022. Economic, technical, operational, and geographical parameters were evaluated during the system design and optimization. Eight distinct systems, derived from various source combinations, were designed. A multi-criteria decision analysis (MCDA) technique, considering power output, net present cost (NPC), the levelized cost of electricity (LCOE), and greenhouse gas (GHG) emissions was employed to determine the most reliable and sustainable system for the specified location. The highest ranking optimal system comprised a hybrid of solar PV, wind turbine, hydro turbine, and battery bank. This system not only championed economic efficiency with an NPC of $166,173.78 and an LCOE of 0.14$/kWh but also stood out as an environmental steward with zero GHG emissions. In stark contrast, the traditional system of the diesel generator and the PV/generator ranked last, both economically and environmentally, with NPCs of $425216 and $397445, LCOEs of 0.36$/kWh and 0.32$/kWh, and GHG emissions of 86168 kg/year and 72097 kg/year, respectively.

Keywords Hybrid energy · HOMER Pro · Net present cost · Cost of electricity · Emission analysis

✉ Shayan Tariq Jan
Shayantj11@yahoo.com

[1] Department of Energy Engineering Technology, University of Technology, Nowshera 24100, Pakistan

[2] Department of Electrical Engineering, College of Engineering, Northern Border University, 73222 Arar, Saudi Arabia

[3] Department of Electrical Engineering, College of Engineering, Jouf University, 72388 Sakaka, Saudi Arabia

Published online: 09 January 2024

1 Introduction

Reliable and sustainable electric power sources have become an absolute necessity for a nation to prosper, grow, and develop in this era of technology (Zameer & Wang, 2018). From the smallest task of a toothbrush to the gigantic task of powering industries, all rely on electricity, making it a basic need of life. Presently, earth's population has crossed 7 billion and is rapidly on the rise causing an increase in electricity demand (Coyle & Simmons, 2014). The largest contributor to the electrical energy mix is fossil fuels whose reserves are rapidly declining due to their excessive use (Awan et al., 2022). The difference in supply and demand of fossil fuel has caused its price to skyrocket. This utilization of fossil fuels is also escalating the quantity of greenhouse gases in the earth's atmosphere which are highly toxic and harmful to the environment and living beings (Chisale & Mangani, 2021; Turkdogan, 2021). These factors are leading the earth toward energy scarcity and crisis.

Pakistan is located in South Asia with a population of over 225 million. Since 2006, it has been facing an energy crisis where the electricity supply and demand are not being met. The country produces 60% of its electricity from fossil fuel-based thermal power plants (Khan et al., 2020). Pakistan has a total energy demand of about 25,000 MW but a distribution capacity of approximately 22,000 MW, creating a gap of 3000 MW which rises to 6000 MW in peak summers (Iqbal et al., 2021). This has led to many industries shutting down across the country. This situation has drastically impacted the county's development.

About 62.5% of Pakistan's population lives in rural areas where the energy crisis is even more severe. Those areas receive electricity of low quality with load sheading durations reaching 18 h per day. A study showed that about 60% of Pakistan's land has no access to the National Distributing Power Grid, impacting the quality of life drastically (Ur Rashid et al., 2022). This has led to an urgent need for alternate power sources for the country.

Pakistan, located at latitudes 24° and 27° N and longitudes 61° and 76° E (Rafique & Rehman, 2017), occupies a strategic geographical position that blesses it with a wealth of renewable energy potential (Wang et al., 2020). This potential is a viable asset in the face of mounting energy crises and global calls for sustainable energy solutions. The renewable resources at Pakistan's disposal are solar, wind, hydro, biomass, and geothermal energy. Each of these sources presents unique opportunities and challenges, but collectively, they paint a promising picture of the country's energy future. Comprehensive studies by the Pakistan Meteorological Department (PMD), the National Renewable Energy Laboratory (NREL), the Alternative Energy Development Board (AEDB), and data from NASA's weather satellite have mapped out the distribution of these renewable energy sources across the nation's diverse topography (Dincer, 2011).

Wind energy finds its niche in Pakistan's vast wind corridors, with a theoretical installed power capacity potential of 346 GW (Sumair et al., 2020). Along with wind, the sun's radiant energy offers another avenue for sustainable power. Most parts of Pakistan have an average daily solar radiation of 5 kWh/m^2/day, translating to a solar potential of 2900 GW (Solangi et al., 2019). Such figures not only highlight the abundance of solar energy but also underscore the need for robust infrastructure and policies to harness it. Hydropower, a cornerstone of Pakistan's energy landscape, currently contributes to about 30% of the nation's electricity. Yet, even with such significant contributions, there remains an untapped hydro energy potential of over 40,000 MW (Uddin et al., 2019). This indicates both the vastness of Pakistan's hydro resources and the opportunities that lie ahead.

Despite these abundant resources, the current energy landscape in Pakistan is still in its early stages when it comes to fully embracing renewables. Excluding hydro, renewables

account for a mere 6% of the country's energy mix (Wang et al., 2020). This gap between potential and utilization underscores the pressing need for strategic investments, policy reforms, and public–private partnerships. By capitalizing on its renewable resources, Pakistan can not only address its energy challenges but also position itself as a leader in sustainable energy in the region.

Choosing the optimal renewable energy source for a particular location is a multifaceted endeavor, because of the unique characteristics and constraints of the site in question. A wide range of factors, ranging from the availability of resources and infrastructural prerequisites to potential environmental repercussions and stakeholder interests, collectively shape the feasibility landscape of renewable energy initiatives. However, relying solely on a single renewable energy source often falls short of delivering a cost-effective and consistent power supply (Ahmed et al., 2021). The inherent variability of renewable energy, dictated by ever-fluctuating climatic and geographical conditions, presents challenges (Sawle et al., 2018). For instance, solar energy, while abundant during daylight hours, decreases as night approaches. Hydro energy, on the other hand, might surge during summer months, only to diminish during drier winter spells. Wind energy, too, faces the same issue. Certain days they witness low wind speeds, rendering them insufficient for power generation. This inherent inconsistency underscores the rising importance of hybrid systems, where multiple energy sources work in combination, compensating for each other's periodic shortfalls (Al-Badi et al., 2022; Islam et al., 2022).

To maximize the performance of hybrid systems site assessment is of vital importance. Such an assessment should analyze factors like solar radiation potential, wind patterns, land accessibility, proximity to existing grid infrastructure, and the nuances of local regulatory edicts. Having a comprehensive insight into these factors, decision-makers can optimize renewable energy deployments and ensure their longevity.

However, merely identifying potential energy sources is just one piece of the puzzle. To truly prioritize renewable technologies that resonate with sustainability, a comprehensive evaluation is imperative. Multiple-criteria decision-making (MCDM) is an important tool in renewable energy selection. It equips stakeholders with a structured framework to juxtapose renewable energy alternatives against a set of predefined criteria. The methodology is systematic, involving the delineation of pertinent criteria, weight allocation based on their significance, comparative analysis of renewable options, result aggregation, and subsequent sensitivity analysis.

The true strength of MCDM lies in its ability to offer a transparent mechanism that contemplates variables like cost-effectiveness, environmental footprint, scalability potential, and reliability metrics. By using MCDM, stakeholders are better positioned to make decisions that not only align with their overarching objectives but also acknowledge the intricate interplay and trade-offs intrinsic to renewable energy selections.

A rigorous evaluation of hybrid renewable energy sources complimented with MCDM methodologies forms the foundation of informed decision-making and the realization of renewable energy ventures. By utilizing these methodologies in its strategic tapestry, Pakistan stands poised to not only tap into its vast renewable energy reservoirs but also champion the cause of environmental sustainability.

In this paper, the main aim is to design an optimized hybrid power system that can meet the load demand (20 kW) for the small rural community of Bankhwar Utrar in Kalam, northern region of Pakistan. Bankhwar Utrar was selected due to its limited access to the national grid and exposure to the high potential of renewable energy sources (Sheikh, 2009). Amidst the backdrop of inconsistent power quality and prolonged power outages, four primary power sources emerge and are selected for the hybrid system: the traditional

diesel generator, the solar PV panels, the wind turbines, and the relentless hydro turbines. Utilizing HOMER Pro, the study models eight distinct hybrid energy systems, each a unique amalgamation of the aforementioned sources. To truly identify the best system, the MCDM technique is used (Basheer et al., 2022; Bohra et al., 2021). Through MCDM, each system is evaluated against a set of pivotal criteria: power output consistency, the economic feasibility gauged through net present cost (NPC) and the levelized cost of electricity (LCOE), and the environmental footprint measured by greenhouse gas (GHG) emissions. This comprehensive assessment aims not just to identify a system that powers the community but to unveil one that is reliable, sustainable, and resonates with the ethos of environmental stewardship. This paper illuminates the path toward a future where energy is not just available but is sustainable, reliable, and harmonious with nature for rural communities like Bankhwar Utrar.

The main contributions of the paper are as follows:

- Designing a hybrid energy system with optimal cost and capacity to electrify a rural village with limited access to electricity.
- Investigating the techno-economic performance of the 8 different HES designed from PV/wind/hydro/generator/battery through Homer Pro.
- Comparative study of the proposed systems based on the energy produced, NPC, COE, and GHG emissions.
- Comparison of the cost of extension of the grid to the stand-alone configuration
- Ranking of the systems through MCDM based on technical, economic, and environmental criteria.

1.1 Literature review

The quest for optimal energy solutions using hybrid systems has been the focus of numerous studies globally. Ali et al. embarked on an exploration of the potential of hybrid energy systems in Dera Ismail Khan, Pakistan (Ali et al., 2021a). Their objective was to assess the viability of photovoltaic (PV) systems in comparison to other renewable energy sources in the region. Through their study, it was discerned that PV systems exhibited remarkable potential, a trend further augmented by the declining costs of PV technology. This observation was paralleled by the government's initiatives in commissioning large-scale PV projects, as well as the rising demand for small-scale residential and commercial installations.

Transitioning to another part of the country Pindiali, KPK, Pakistan, a pivotal study was carried out to determine the most efficient energy system for a 600 kW load using HOMER Pro (Adil Khan et al., 2019). Their methodology involved a comprehensive evaluation of individual and hybrid energy configurations. The key findings highlighted that a PV, wind, and battery hybrid system was superior, with a notable NPC of $13286, OC of $184.6, and LCOE of $0.15/kWh.

In a similar context, but shifting the geographical focus to the terrain of Gilgit-Baltistan in Pakistan was the focus of another comprehensive study by Ali et al., where hydroelectric power emerged as the dominant renewable energy source, suggesting its potential amplification with wind and battery backup systems (Ali et al., 2021b). These studies show that Pakistan has a vast potential for harnessing renewable energy resources, with significant variations based on regional geographies and climatic conditions. From the arid landscapes of Dera Ismail Khan to the mountainous terrains of Gilgit-Baltistan, the adaptability and versatility of hybrid systems are evident. Moreover, the declining costs of PV technology,

combined with the government's proactive initiatives, have positioned Pakistan on the trajectory of a sustainable energy transition. Yet, it is essential to recognize that while hybrid systems offer promising solutions, the optimal configuration is highly contingent on the unique environmental and geographical conditions of each location. Therefore, the emphasis should be on localized energy solutions that not only cater to immediate energy demands but also ensure long-term sustainability and environmental conservation.

The same analysis can be done throughout the world, irrespective of country as renewable energy sources depend on the geographical location. Transitioning to another part of Asia, Nesamalar et al. (2021) carried out a study in Virudhunagar, India, focusing on designing a PV system for a college. Both on-grid and off-grid systems were scrutinized. The key finding was that a stand-alone PV system was inadequate for the college's energy needs. While the off-grid system highlighted the efficacy of a hybrid PV/generator configuration, the on-grid system pinpointed batteries as the optimal solution. This study reinforces the pivotal role backup systems play in ensuring continuous power supply in isolated settings.

Moving further east to Delhi, India, Kumar and Tewary (2022) designed a stand-alone hybrid energy system (HES) to cater to a 5 kWh/day load. Their research illustrated that renewable energy sources could meet an impressive 98% of the load requirement, with the residual 2% catered to by the generator. A salient observation was the system's capability to produce a surplus of 12% more energy than the stipulated load requirement. A recent study delved into the role of the Internet of Things (IoT) in acting as a sustainable energy management solution specifically tailored for Indian tourism destinations (Tiwari et al., 2022). The emphasis was not only on the technology itself but also on the awareness and adaptability of the tourism personnel toward Energy Management. The study utilized the Seroquel method to gauge the effectiveness of IoT in addressing sustainable energy demands. Preliminary findings from the study echoed the larger narrative of the need for adopting advanced technologies in traditional spaces.

In a similar context, but shifting the geographical focus to Sumatra Island, Indonesia, Riayatsyah et al. (2022) delved into the intricacies of a hybrid system of PV/wind for a university. The combined PV/wind system was found to satiate only 82% of the university's energy demand. To bridge this gap, the researchers proposed batteries and grids as potential backup solutions, emphasizing the significance of backup sources in renewable energy systems.

Meanwhile, in northeastern Nigeria, a parallel study was conducted to discern the ideal energy configuration for a school (Salisu, 2019). The optimal design was a hybrid solar PV battery system with an NPC of $18,161 and a LCOE of $0.233/kWh. However, the addition of a wind turbine proved counterproductive, reinforcing that system efficacy is intrinsically tied to specific geographical and climatic conditions. This shows that a system designed for one location may not perform at the same level when the location is changed because of different climates and geographical conditions (Sadat et al., 2020).

Seedahmed et al. shifted the focus to Al-Shumaisi, Saudi Arabia, with their study aiming at designing an HES for a remote company bereft of grid power access (Seedahmed et al., 2022). The researchers illustrated that an HES, in contrast to a sole diesel generator, could diminish the net present cost by 13.84% and substantially curtail greenhouse gas emissions by 64.2%.

Similarly, AKAN et al. in Tekirdağ, Turkey, designed a HES encompassing PV, wind, and battery components for an 11.2 kWh/day load (Akan, 2021). Their study showcased that the system adeptly met the load requirements, with energy sources contributing differentially: PV at 62% and wind at 38%.

Rad et al., in their study in Northwest Iran, proposed a hybrid energy system (HES) consisting of PV, wind, biogas, and fuel cells for a 360 kWh/day demand (Rad et al., 2020). Their system, with a COE of 0.233 $/kWh, was rooted in the synergies between solar, wind, and biogas. Hoseinzadeh et al. explored a similar hybrid avenue in Catania, Italy, where PV contributed a significant 72% of the total power output (Hoseinzadeh & Astiaso Garcia, 2022). The studies highlighted that utilizing a mixture of renewable sources drastically reduced the LCOE and provided reliable sustainable power.

Malaysia witnessed a comparative study spanning three rural locations: Pontian, Kerteh, and Teluk Intan (Wahid et al., 2019). Each location was assessed with the same power-rated stand-alone systems of biomass, wind, and solar PV. While biomass consistently achieved an LCOE of $0.342/kWh, the performance of solar and wind varied, emphasizing the importance of localized conditions. In a distinct geographical setting, in Peru, researchers explored the hybrid potential of diesel, wind, and PV across three locations (Rinaldi et al., 2021). Each location demonstrated unique energy preferences, emphasizing the intricate interplay between geographical conditions and energy system efficacy. Shifting the spotlight to Europe, an intriguing study recently explored the intersection of renewable energy awareness and expectations within European Union households (Rosak-Szyrocka et al., 2023). In this comprehensive research spanning seven countries, including the Czech Republic, Slovenia, and Germany, to name a few, a qualitative examination was conducted with over 17,030 respondents from April 2021 to June 2022. It emerged that while households acknowledged the environmental benefits of renewable energy, such as the reduction in CO_2 emissions, their awareness remained relatively low. Interestingly, there was a reluctance in willingness to pay more for services, even if those services employed renewable energy sources. The study also highlighted an underlying apprehension among respondents about the potential drawbacks of certain renewable sources, like wind energy, which they perceived might mar landscapes and impact tourism adversely.

As the world grapples with the dual challenges of climate change and energy security, the role of multiple-criteria decision-making (MCDM) becomes paramount in evaluating and implementing hybrid renewable energy systems. MCDM offers a robust framework to make informed decisions by considering multiple criteria that span across technical, environmental, and socioeconomic realms, ensuring a holistic approach to energy system selection. Addressing the growing emphasis on sustainable energy solutions, Baseer et al. employed an MCDM approach combined with GIS modeling to determine wind farm site suitability in Iran (Rinaldi et al., 2021). Their methodology was intricate, factoring in wind resources, accessibility, and various climatic, economic, and esthetic criteria. The findings underscored the immense potential of Saudi Arabia for wind energy projects.

In Yanbu, Saudi Arabia, Kharrich et al. delved into the economic aspects of hybrid microgrids, drawing attention to the potential of PV, wind, and biomass systems when combined with energy storage (Baseer et al., 2017). Almasad et al.'s study provided a framework for implementing PV solar power projects in Saudi Arabia, intertwining technical, environmental, and economic considerations (Kharrich et al., 2021). The researchers adeptly harnessed the AHP in conjunction with the PROMETHEE to ascertain site suitability.

Wang et al.'s study took a distinct approach, evaluating four energy distribution systems: gas turbine, fuel cell, PV, and combustion engine (Almasad et al., 2023). Utilizing the combined prowess of DEMATEL and VIKOR, they concluded that the photovoltaic scenario was the most beneficial. This was further buttressed by research from Dehghan et al., who employed GIS and MCDM to pinpoint the optimal location for a wind farm in Iran, consolidating the value of MCDM in energy system research. The role of MCDM in the

realm of renewable energy system selection is undeniable. As the studies reviewed herein showcase, MCDM techniques, when adeptly applied, can guide policymakers, researchers, and practitioners in making informed choices that align with both environmental sustainability and economic viability. The multi-dimensionality of energy decisions, encompassing technical, environmental, and economic facets, underscores the indispensability of MCDM in charting a sustainable energy future.

Table 1 provides a comparative analysis of all the above-discussed studies, highlighting the key findings and limitations.

In conclusion, the myriad studies underscore the significance and versatility of hybrid energy systems. They not only demonstrate the potential of these systems but also emphasize the necessity for location-specific optimization. As the quest for sustainable energy solutions intensifies, these studies provide invaluable insights, paving the way for future innovations.

2 Methodology

HOMER is designed to analyze the proposed hybrid energy system for selected locations based on power output, CO_2 emissions, NPC, and LCOE (Kavadias & Triantafyllou, 2021). The hybrid energy system must be able to serve the target location's load. Renewable energy sources are possible inputs to the HOMER. It performs the optimization analysis and generates results after considering all of the load and resource inputs. HOMER sets the system in several configurations using various combinations of the components used and performs an energy balance for each of these configurations. HOMER analyzes the feasibility of each of these setups by determining if the load demand is satisfied under defined conditions. It also calculates the installation, operating, and maintenance costs during the project's lifetime (Mahesh & Sandhu, 2020). Figure 1 depicts the flowchart of the approach used to build the proposed hybrid energy systems and select the best one based on MCDA (Ammari et al., 2022; Chen et al., 2022).

2.1 Net present cost (NPC)

The NPC tells a user about the finances involved in the project during its lifetime. It takes in to account the initial capital cost of the project, the operation and maintenance cost, the replacement cost, and the salvage value as shown in Eq. (1)

$$\mathrm{NPC} = \boldsymbol{\Sigma}(C_{\mathrm{capital}} + C_{\mathrm{operation\ \&\ maintenance}} + C_{\mathrm{replacement}} - C_{\mathrm{Salvage}}) \tag{1}$$

where C_{capital} is the initial investment cost, $C_{\mathrm{operation\ \&\ maintenance}}$ is the running cost, $C_{\mathrm{replacement}}$ is the replacement value, and C_{Salvage} is the salvage value.

HOMER uses Eq. (2) to calculate the NPC of the project (Shezan et al., 2022)

$$\mathrm{NPC} = \frac{C_{\mathrm{ann}}}{\mathrm{CRF}\left(i \cdot R_{\mathrm{pro}}\right)} \tag{2}$$

where C_{ann} is the annualized cost, CRF is the capital recovery factor, i is the annual interest rate, and R_{pro} is the project lifetime.

Table 1 Comparative analysis of discussed studies

Sources	Methodology	Focus Area	Key findings and figures	Limitations
PV/wind/biomass/battery (Sheikh, 2009)	HOMER	Pindiali, KPK, Pakistan	Best operating system for 600 kW load was PV, wind, and battery with NPC of $13286, OC of $184.6, and LCOE of $0.15/kWh	System location-specific; Biomass had high running cost
PV/wind/biomass/battery (Basheer et al., 2022)	HOMER	School in northeastern Nigeria	Optimal system was hybrid solar PV battery with NPC of $18161 and LCOE of $0.233/kWh	Wind turbine addition was not efficient
PV/wind/biomass/(Ali et al., 2021a)	HOMER	Three rural locations in Malaysia	Biomass had a consistent LCOE of $0.342/kWh across locations. PV and wind LCOE varied, with Kerteh having the lowest	Results varied across cities due to geographical differences
Diesel/wind/PV (Adil Khan et al., 2019)	HOMER	Three locations in Peru	Each location demanded different designs: Campo Serio favored wind, El Potrero favored solar, and Silicucho preferred diesel	System design and costs varied across locations
PV/wind/biogas/fuel cell (Tiwari et al., 2022)	HOMER	Northwest rural city of Iran	Solar/wind/biogas system most feasible with COE of 0.233 $/kWh	Off-grid expensive than on-grid systems due to proximity to the power grid
PV/wind/fuel cell/electrolyzer/hydrogen tank (Riayatsyah et al., 2022)	HOMER	Island city of Catania in Italy	PV/wind system complemented each other in a hybrid model among PV/wind/fuel cell/electrolyzer/hydrogen tank. PV contributed 72% of total power	Wind Turbine has the least production/efficiency
Hydro/wind/PV/DG/Battery storage (Salisu, 2019)	HOMER	Northern province of Gilgit-Baltistan in Pakistan	Hydroelectric power had the highest potential. Integration of wind and battery backup systems further optimized the output	PV was the least effective in the region Independent DG sources produced high GHG and high operating cost
PV/wind/biomass/grid (Ali et al., 2021a)	HOMER	Dera Ismail Khan, Pakistan	PV systems exhibited significant potential compared to other renewable energy sources in the region	Regional climate did not suit other sources. Wind and biomass are ineffective due to low source

Table 1 (continued)

Sources	Methodology	Focus Area	Key findings and figures	Limitations
PV/battery/generator/grid (Nesamalar et al., 2021)	HOMER	College in Virudhunagar, India	Hybrid PV/generator was effective off-grid, while on-grid required PV/battery/grid	Stand-alone PV system insufficient. College specific energy needs
PV/wind/battery/grid (Riayatsyah et al., 2022)	HOMER	University on Sumatra Island, Indonesia	Combined PV/Wind system fulfilled 82% of demand, indicating a need for backup. Grid were identified as solutions with low COE of 0.044$/kWh	Individual RE sources are not efficient to fulfill demand 100% renewable systems increase the COE to 0.060 $/kWh
Wind/PV/DG/Battery Storage (Kumar & Tewary, 2022)	HOMER	Delhi, India	Optimized system produced 19.3% more than the demand. COE of 0.393 $/kWh. Cost can be reduced with on-grid systems to compensate for DG and battery	Limited to a 5 kWh/day load in Delhi. generator supplemented 2%, leading to GHG
Wind/fuel cell/DG/battery (Seedahmed et al., 2022)	HOMER	Al-Shumaisi, Saudi Arabia	Wind/fuel cell/generator/battery system reduced NPC by 13.84% and greenhouse gas emissions by 64.2% compared to a diesel generator	Battery increases cost. Independent DG system has a high running cost. Independent DG sources produced high GHG
PV/wind/battery (Akan, 2021)	HOMER	Tekirdağ, Turkey	PV, wind, and battery met 11.2 kWh/day load. PV supplied 62% energy, wind turbine 38%. Optimized system reduced cost COE of 0.409 $/kWh	Individual RE sources are not efficient to fulfill demand Battery increases cost and reason for higher COE
PV/Wind/DG (Hoseinzadeh & Astiaso Garcia, 2022)	HOMER	Peru	Optimized systems in different locations produced different results COE: 0.47$/kWh (Campo), 0.460$/kWh (El Potrero) and 0.504 $/kWh (Silicucho)	On-grid systems are more expensive Individual RE sources are not efficient

Table 1 (continued)

Sources	Methodology	Focus Area	Key findings and figures	Limitations
Wind/generator/battery (Rinaldi et al., 2021)	GIS and MCDM	Wind farm site in Iran	Identified Izadkhast as the optimal location for wind farm considering multiple factors. Optimized system and ideal location reduced COE to 0.0719 $/kWh	Require large area for the wind farm. Specific to wind farm feasibility in Iran
Gas turbine, fuel cell, PV, combustion engine (Baseer et al., 2017)	DEMATEL and VIKOR		PV scenario emerged as the best alternative among the evaluated energy distribution systems	General evaluation without specific location
Wind/generator/battery (Kharrich et al., 2021)	MCDM and GIS	Wind farm site in Saudi Arabia	Identified Ras Tanura, Turaif, and Al-Wajh as most suitable wind farm sites. Central and southeastern regions were unsuitable	Specific to wind farm feasibility in Saudi Arabia
PV/biomass (Almasad et al., 2023)	GPC algorithm	Yanbu region of Saudi Arabia	Hybrid microgrid was optimal for Yanbu. The PV system had larger size than biomass	Running cost due to constant biomass supply

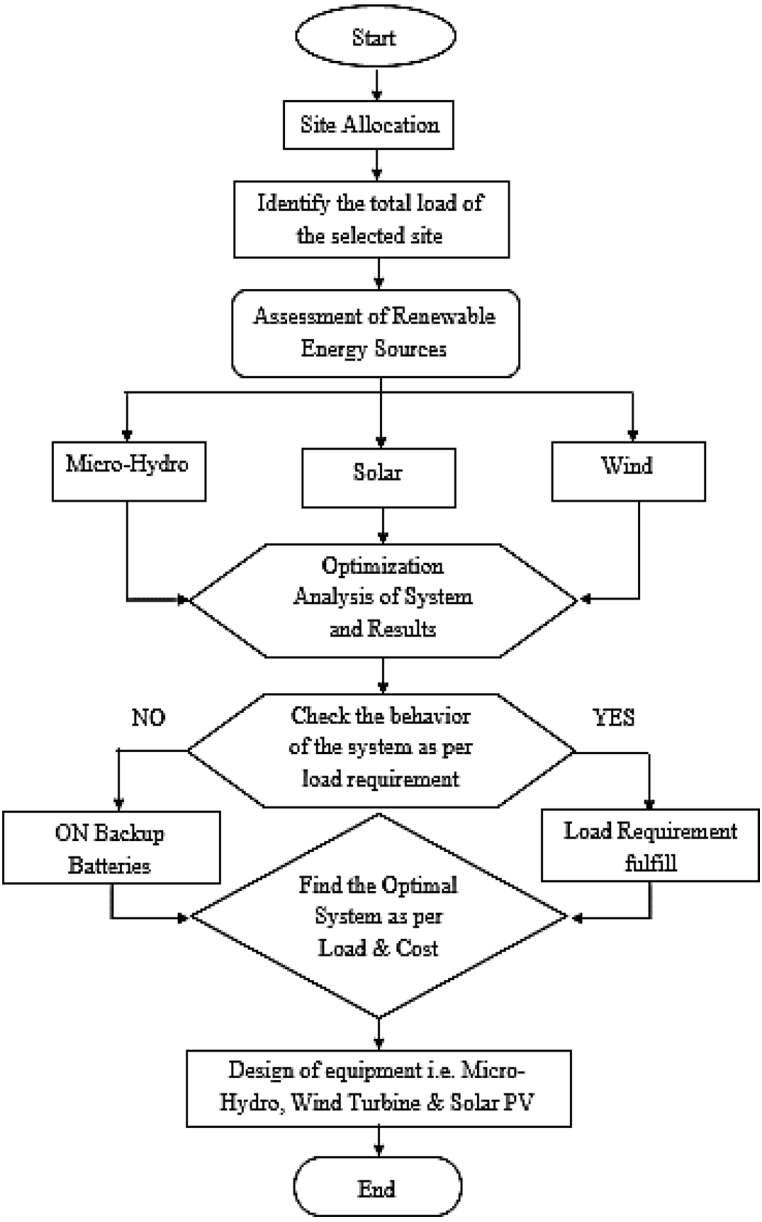

Fig. 1 Methodology flowchart

2.2 Levelized cost of electricity (LCOE)

LCOE of a system tells us about the cost of electricity per kWh of the designed system. It depends on the cost of the designed system, the electrical energy produced, and the load as shown in Eq. 3 (Shezan et al., 2022).

$$\mathrm{LCOE} = \frac{C_{\mathrm{ann}}}{E_{\mathrm{prim}} + E_{\mathrm{def}} + E_{\mathrm{grid}}} \tag{3}$$

where E_{prim} is the total primary load, E_{def} is the differed load, and E_{grid} is the energy given to the grid.

2.3 Total annualized cost

The sum that is calculated yearly while the project is being evaluated, and supplied the NPCs required to satisfy the part income request is known as total annualized cost. The overall annual cost is determined using the NPC and raised with the capital recovery factor, utilizing Homer Ace programming.

2.4 System design

The energy sources selected for the hybrid systems were diesel generator, solar PV, wind, batteries, and hydro. The diesel generator is included in the study because it is quite popular in the local community and the go-to source for backup power during electricity load shedding. The diesel generator is taken as the base case for the study. Using HOMER, eight different systems were designed and analyzed in detail. For each system, the most reliable, sensible, and cost-effective options were selected to fulfill necessary load requirements. The following is a list of the eight different systems that were designed for the hybrid renewable system:

- System 1: Diesel generator
- System 2: Diesel generator and hydro
- System 3: Diesel generator and PV
- System 4: Diesel generator and wind
- System 5: Hydro, wind, and batteries
- System 6: Hydro, PV, and batteries
- System 7: Wind, PV, and batteries
- System 8: Hydro, wind, PV, and batteries.

The microgrid has AC and DC buses. The PV and backup batteries in the system are DC sources connected to the DC bus while the hydro, wind, and generator are AC sources connected to the AC bus as shown in Fig. 2. The load is also considered as AC. A power converter is used in the system so that the DC power can be converted to AC power for the load. It can also convert AC to DC for charging the batteries.

3 Site selection

The economic and technological feasibility of any renewable energy-based power project is dependent on selecting a suitable site. The availability of renewable energy sources such as solar, wind, and hydro in the preferred area, as well as the electric load to be met, must be considered. The first phase in any successful project is to choose a location and design suitable system components according to its strengths and weaknesses. The location selected is Bankhwar Utrar, which is situated at coordinates 35°29.4'N, 72°34.8'E in Pakistan's

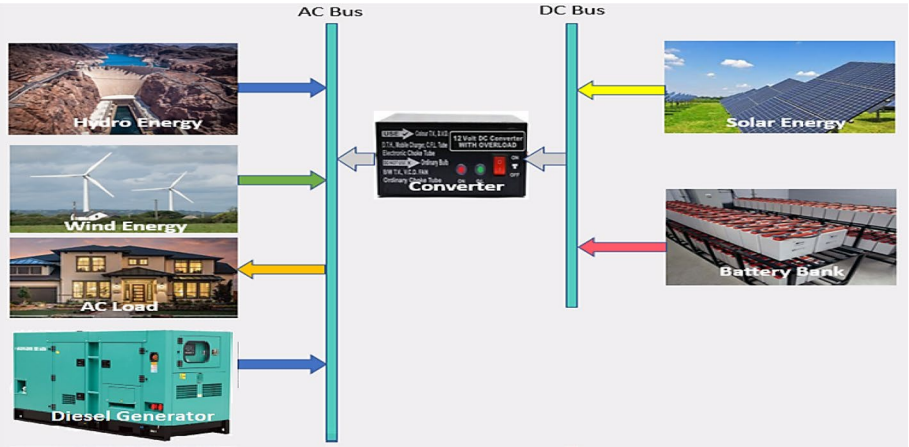

Fig. 2 Energy sources are connected to the grid

Khyber Pakhtunkhwa province. The location has the advantage of being situated on the bank of a stream from the Swat River which gives the option to utilize a microhydro-based hybrid energy project. The selected region is a small community of a few hundred people. Figure 3 depicts the projected site.

According to the latest census, the total number of households counts to 28 with 178 inhabitants. The ratio of the population of male/female is 53.80%/46.19%, with a yearly population growth rate of 1.86%. The major occupations of the locals include fisheries, cattle breeding, cultivation, and construction. The main resources for cooking and heating are wood and kerosene oil, while illumination is arranged through kerosene oil lamps (Al-Badi et al., 2022). Diesel power generators and gas are used as fuel by the population for light, cooking, and heating.

Kalam district has become the focal point for tourism due to its natural beauty. However, the region is still deprived of basic electrification, and large portions of the area are not integrated with the national grid of Pakistan (Sawle et al., 2018). Some regions are fed by Pakistan National Grid but that does not fulfill the requirements due to the countries'

Fig. 3 Projected site

supply-side constraints (Sawle et al., 2018). Bankhwar Utrar being a rural small village has not a proper connection with any grid and hence has been deprived of electricity. Connecting it with the grid requires high investment and infrastructure, making it the potential site for the on sight renewable power generation.

3.1 Climate condition

According to the Meteorological Department, Kalam has a humid subtropical climate with slightly warm temperatures (Ahmad et al., 2012). Kalam has an annual precipitation of 639 mm and a mean temperature of 13.4 C. The wettest month is April, with 93 mm of precipitation. The driest month is November, with 15mm of precipitation. July is the warmest month of the year, with an average temperature of 24.1 °C. January has the coldest average temperature of 1.5 C. Figure 4 depicts the climate data for the region.

3.2 Resource availability

It is necessary to determine the capability of various energy resources to model an electrical system for meeting the load requirement of the proposed location. A field visit was made to identify the possibility of microhydro at the proposed site, and the height required of the head. The stream flow rate was collected from the Khyber Pakhtunkhwa Irrigation Department at the location. By entering the location's coordinates, annual monthly sun global horizontal radiation, clearance index, and wind speed statistics are obtained from NASA's Surface Meteorology and Solar Energy database website.

3.2.1 Solar irradiance

Solar radiation data are obtained by entering the location's coordinates into HOMER's built-in function for collecting solar data from NASA's Surface Meteorology and Solar Energy databases. HOMER utilizes global horizontal irradiance (GHI) for solar PV outputs, which is the summation of direct normal irradiance (DNI), diffused light, and reflected light. HOMER uses the following calculation to compute the global radiation incidence on the PV array.

Climate data for Kalam												
Month	Jan	Feb	Mar	Apr	May	Jun	Jul	Aug	Sep	Oct	Nov	Dec
Average high °C (°F)	5.3 (41.5)	6.9 (44.4)	12.3 (54.1)	18.2 (64.8)	23.1 (73.6)	29.5 (85.1)	30.5 (86.9)	29.4 (84.9)	26.0 (78.8)	21.2 (70.2)	15.0 (59.0)	8.1 (46.6)
Daily mean °C (°F)	1.5 (34.7)	2.8 (37.0)	7.6 (45.7)	13.0 (55.4)	17.3 (63.1)	23.0 (73.4)	24.1 (75.4)	23.4 (74.1)	19.8 (67.6)	15.1 (59.2)	9.5 (49.1)	4.0 (39.2)
Average low °C (°F)	−2.2 (28.0)	−1.3 (29.7)	3.0 (37.4)	7.9 (46.2)	11.6 (52.9)	16.6 (61.9)	17.8 (64.0)	17.5 (63.5)	13.7 (56.7)	9.0 (48.2)	4.1 (39.4)	0.0 (32.0)
Average rainfall mm (inches)	49 (1.9)	66 (2.6)	88 (3.5)	93 (3.7)	64 (2.5)	32 (1.3)	66 (2.6)	66 (2.6)	41 (1.6)	28 (1.1)	15 (0.6)	31 (1.2)

Fig. 4 Climate data of Kalam (Akan, 2021)

$$\overline{G}_T = \left(\overline{G}_b + \overline{G}_d A_i\right) R_b + \overline{G}_d (1 - A_i)\left(\frac{1 + 2cos\beta}{2}\right)\left[1 + f\, sin^3\left(\frac{\beta}{2}\right)\right] + \overline{G}_{\rho g}\left(\frac{1 - 2cos\beta}{2}\right) \tag{4}$$

where $\overline{G}_T$ is the average of global horizontal radiation on the earth's surface throughout the time step kw/m^2], $\overline{G}_o$ is beam radiation [kw/m^2], $\overline{G}_d$ is diffuse radiation [kw/m^2], b is the slope of the surface [°], and ρ_g, also called albedo, is ground reflectance [%].

Figure 5 displays solar radiation data collected from NASA's Surface Meteorology website using HOMER Pro Software and the location's coordinates. The highest sun radiation is 7.080 KWh/m^2/day in June, while the minimum solar radiation is 2.440 Kwh/m^2/day in December.

Figure 5 demonstrates that the daily radiation is greater than 5.5kWh/m^2/day during April, May, June, July, August, and September due to higher sun shine hours than in other months. The yearly average solar radiation is 5.05 kWh/m^2/day. The months with abundant solar irradiance coincide with periods of higher energy demand, especially in regions with seasonal variations in climate. The consistent daily solar radiation exceeding 5.5 kWh/m^2/day during the mentioned months indicates that Bankhwar Utrar has a robust solar resource. This resource can be harnessed effectively for solar PV technologies (Jan & Noman, 2023).

3.2.2 Wind Resource

HOMER uses wind speed data in meters per second (m/s) from NASA's Surface Meteorology and Solar Energy database, averaged monthly over ten years and measured at 50 m anemometer height. The HOMER was used to set the hub height in the projected hybrid system to 30 m. The hub height tends to rise as the wind speed rises. HOMER uses Eq. 5 power law profile to compute wind speed at the hub height.

$$V_{\text{hub}} = V_{\text{anem}}\left(\frac{Z_{\text{hub}}}{Z_{\text{anem}}}\right)^{\alpha} \tag{5}$$

where the wind speed at hub height is expressed as $V_{\text{hub.}}$, the wind speed at anemometer height as $V_{\text{anem.}}$, the hub height is referred to as Z_{hub}, the height of the anemometer is referred to as Z_{anem}, and the power law exponent is given as α.

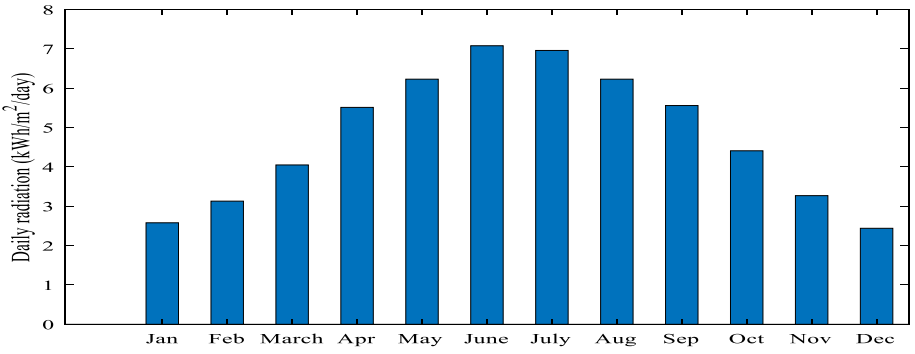

Fig. 5 Solar potential

Monthly wind speed data collected from NASA's Surface Meteorology website using Homer Pro Software are illustrated in Fig. 6. In October, the highest wind speed is 8.30 m/s, while the minimum wind speed is 5.940 m/s in July. The wind speed is more than 6.5 m/s in March, April, May, October, November, and December. The data indicate that the average annual wind speed in Bankhwar Utrar is 6.81 m/s. This average wind speed is a key indicator of the overall wind resource in the region and is crucial for estimating the energy output potential of wind turbines. The presence of consistently high wind speeds in October, along with moderate wind speeds in other months, demonstrates the substantial wind energy potential in Bankhwar Utrar.

3.2.3 Hydro resource

Hydropower is the potential energy in water that is transformed into mechanical energy of the turbine coupled to an electrical generator producing electrical energy. Hydropower is classified according to the available head. In this study, the recommended location is the flow of the stream Bankhwar Utrar village Kalam. Except for January, when cold weather affects the water supply in Bankhwar, water resources are adequate throughout the year. The flow of water is greatest in June, July, and August when rivers overflow owing to ice melting. The monthly streamflow for the full year is depicted in Fig. 7.

3.3 Load assessment

For load estimation (Chen et al., 2022; Silva et al., 2020), a visit to the site was made and data were collected from the local area. The survey comprises the records for the number of houses, electrical load demand, and the financial status of the villagers. There were four types of consumers at the chosen site in Utrar, Kalam: Montessori which consists of schools, mosques, residential loads, and commercial loads. Each customer had a unique load profile. The total aggregated power demand of the sample load is estimated through the Watt-hour calculation of each house per hour per day. The Watt-hour of each house is calculated by multiplying the wattage of electrical appliances by their working hours. The aggregated power demand of each appliance is calculated by adding the watt-hours of the

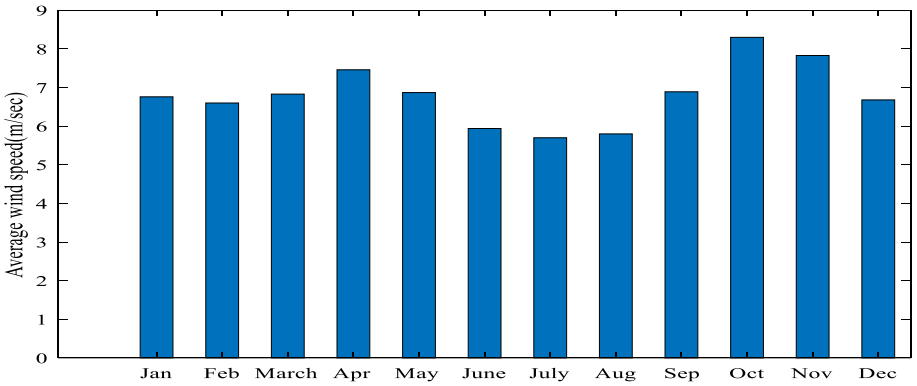

Fig. 6 Wind potential

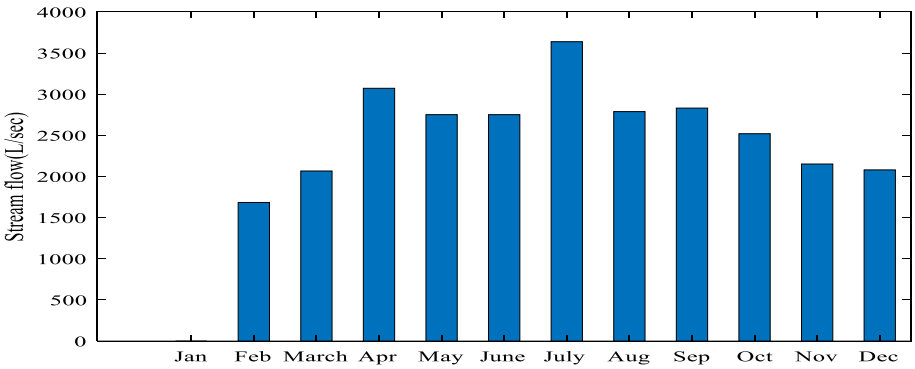

Fig. 7 Hydro potential

appliances used in each household at a particular time (Complete details in Supplementary Data File).

During the demand assessment of the selected sample, mainly two assumptions have been made to represent the seasonal load. For this purpose, the load demand is further classified as "summer load demand" and "winter load demand." The basic difference in both the demands is the seasonal load variations, which is due to fans and water pumps, The demand for fans becomes zero in winter, and water pumps is reduced to half in the winter season while in the summer season; the fans and water pumps are operated at a higher rate comparatively.

3.3.1 Mosque and residential load

For residential load, data were collected from twenty-five homes at the local site and it showed that the load consisted of fans, room lights, safe lights, refrigerators, TV sets, computers, and water pumps (Appendix A, Supplementary Data File). According to the local power substation, the peak loads occur in June and July (Appendix B, Supplementary Data File), whereas off-peak loads are in December and January (Appendix D, Supplementary Data File). In, winter peaks occur from 5 to 9 pm, and summer peaks from 6:30 pm to 11:00 pm. Figure 8a illustrates the residential load profile of Utrar Village.

In the mosque, the load (amplifier, fans, and lights) remains ON only during prayer times (Appendix A, Supplementary Data File). For Fajar prayer, the timing is from 4:00 a.m. to 7:00 a.m. However, the hour of Zuhar prayer is relatively consistent throughout the year, and it is from 12:00 to 14:00. In the summer, from 15:30 to 21:30, three additional prayers, namely Asr, Maghreb, and Isha, for three to four hours; in the winter, from 4 p.m. until 9:30 p.m. The water pump operating times are Fajar and Maghreb. Figure 8b depicts the load profile of mosques.

3.3.2 Commercial and school load

Commercial loads operate between 8 a.m. and 4 p.m. Commercial load demand is highest at 8kW according to the local power substation (Appendix B, Supplementary Data File). Only safety lights are active after working hours. A complete load profile of our proposed site is given, which shows that peak hours occur in noon because of

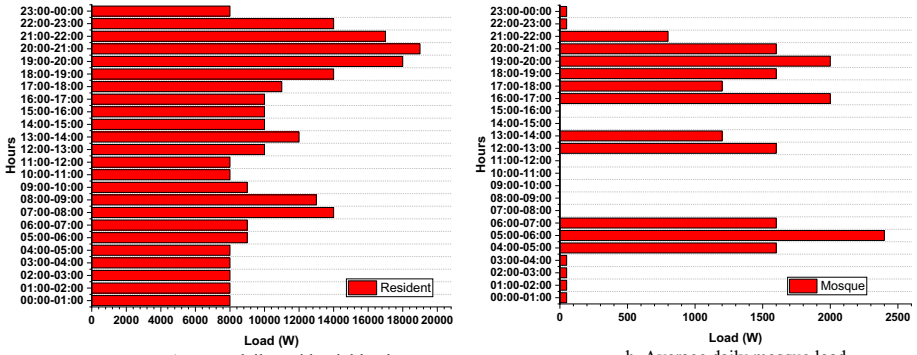

a. Average daily residential load

b. Average daily mosque load

Fig. 8 **a** Average daily residential load, **b** average daily mosque load

commercial peak load and in the evening to night because of residential load peak time. Figure 9a depicts the load profile during peak months.

Winter school hours are 8:00 a.m. to 1:00 p.m., while summer hours are 7:00 a.m. to noon. There are six classrooms, one office, and one teacher's room at the local school. There is one fan and four energy-saving lights in each room and a PC and printer in the office. A water pump is used at school for one or two hours every day. Only two safety lights stay on after school closed for the night until 7:00 a.m. Figure 9b depicts the school's load profile during peak months.

3.3.3 Total load profile

The total load profile for the specified region is presented in Fig. 10. Load changes seasonally with weather variation, therefore a seasonal load profile is necessary. The maximum load of approximately 20 kW is observed at peak hours during summer while the lowest load of 4.5 kW during winter.

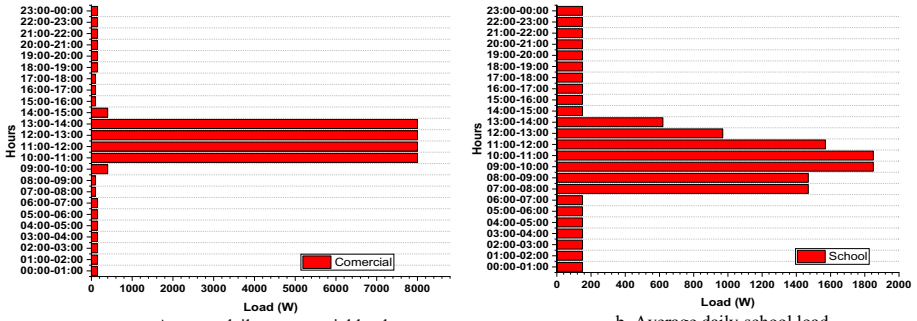

a. Average daily commercial load

b. Average daily school load

Fig. 9 **a** Average daily commercial load, **b** average daily school load

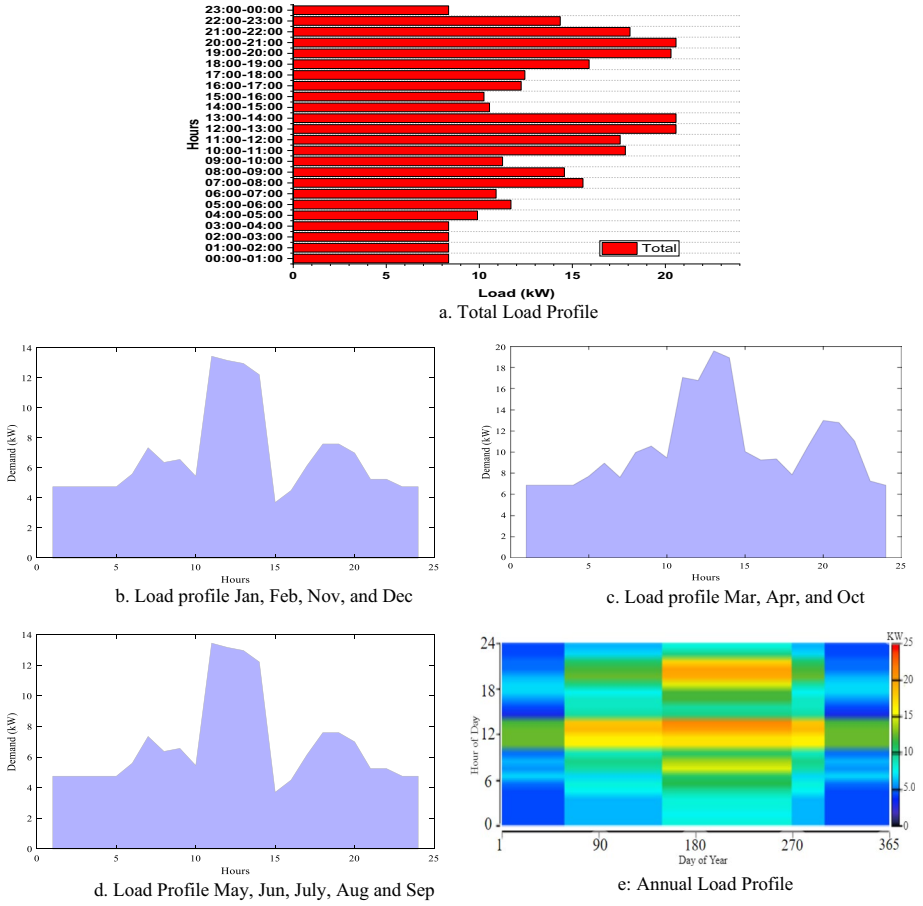

a. Total Load Profile

b. Load profile Jan, Feb, Nov, and Dec

c. Load profile Mar, Apr, and Oct

d. Load Profile May, Jun, July, Aug and Sep

e: Annual Load Profile

Fig. 10 **a** Total load profile, **b** load profile January, February, November, and December, **c** load profile March, April, and October, **d** load profile May, June, July, August, and September, **e** annual load profile

4 Microgrid design calculations and cost function

The design calculations and cost functions for all system components implemented inside this research work are provided in Table 2. The cost is valued at US $ for this study. The maximum peak load of the location is 20 kW in peak summer hours; otherwise, the average load during the day is around 12 kW, reducing to a minimum load of 4.5 kW in winter. Keeping in mind that over time with an increase in population, the load demand will increase, all system designing has been done for an increased peak load of 25 kW instead of 20 kW, while the rest of the loads in other durations have also been increased by 20%.

Table 2 Component cost

Components	Initial cost ($/kW)	Replacement cost ($/kW)	Operating cost ($/kW)	Lifetime (year)
PV panel	350	350	10	25
Wind turbine	6000	5000	25	20
Diesel generator	400	400	0.010	15000h
Hydro turbine	6000	3250	57	25
Battery	4400	1320	8	15
Converter	300	300	0.010	15
Microgrid	8000	160	0.08	

4.1 Solar PV

A PV module is a device that creates direct current power when there is global solar radiation (Tariq Jan & Noman, 2022). Equation (6) can be used to calculate the output power of a PV array (Icaza-Alvarez et al., 2022).

$$P_{\text{pv}} = F_{\text{pv}} Y_{\text{pv}} \frac{G_T}{G_{\text{stc}}} \tag{6}$$

where Ypv is the manufacturer's rated power output at STC which are 1 kW/m^2 solar global radiation at 25 °C with no wind (Jan & Noman, 2022), Fpv is the PV module derating factor, GT is the global solar radiation incident on the PV array at the current time step, and Gstc is the global solar radiation under standard test conditions.

The PV panel rated 400W with 14% efficiency is selected for the study. The derating factor of the PV array is about 80%. The ground reflectance is 20% and the tracking system was set on the vertical axis with continuous adjustment. The cost function of solar PV is shown in Eq. (7).

$$\text{PV}_{\text{NPC}} = \text{PV}_{\text{CC}} + \text{PV}_{\text{ins}} + \sum_{1}^{n} \text{PV}_{O\&M} * T_{lifeTime} + \text{PV}_{\text{rep}} * N_{\text{rep}} \tag{7}$$

where the net present costs, capital costs, costs of installation, costs of operations and maintenance, and cost of replacement for solar PV are $\text{PV}_{\text{NPC,}}$ $\text{PV}_{\text{CC,}}$ $\text{PV}_{\text{INS,}}$ $\text{PV}_{\text{O \& M,}}$ and PV_{REP}, respectively. Capital costs include costs for photovoltaic modules, structural costs, and other components. Labor costs, transportation, and installation costs are included. Annual costs of operating and maintenance where the project time in years is displayed by T lifetime. Replacement expenses comprise any protective or other element that must be replaced after a certain period, whereas N_{REP} constitutes the number of components that must be replaced over the whole life of the project.

4.2 Wind turbine

A wind turbine is a device that converts kinetic wind energy into mechanical power and then into electricity. Wind is passed through swept wind turbine bladders to compute wind turbine output; theoretically, only 59 percent of wind turbine power is extracted (Bet's law). The output of a wind turbine may be calculated using Eq. (8).

$$P_{\mathrm{WTG}} = \left(\frac{\rho}{\rho_{\mathrm{o}}}\right) \cdot P_{\mathrm{WTG,STP}} \tag{8}$$

where P_{WTG}, denotes the power output of a wind turbine in kilowatt-hours (kW), $P_{\mathrm{WTG,\ STP}}$ is the power output of a wind turbine at standard temperature and pressure [kW], P is actual air density in kilograms per cubic meter [kg/m^3], and ϱ, is the density of air at normal temperature and pressure (1.225 kg/m^3).

The "EOCYCLE Eo10" wind turbine of rated power 10 kW with 44% efficiency is selected for the study. It has a lower cut-in speed of about 2.75 m per second while the cutout speed is 20 m per second. The rotor diameter is 15.81 m. All costs necessary for the wind turbine system are shown in Eq. (9).

$$\mathrm{WT_{NPC}} = \mathrm{WT_{CC}} + \mathrm{WT_{ins}} + \sum_{1}^{n} \mathrm{WT}_{O\&M} * T_{\mathrm{lifeTime}} + \mathrm{WT} * N_{\mathrm{rep}} \tag{9}$$

where the net present costs, capital costs, costs of installation, costs of operations and maintenance, and cost of replacement for wind turbine WT are $\mathrm{WT_{NPC,}}$ $\mathrm{WT_{CC,}}$ $\mathrm{WT_{INS,}}$ $\mathrm{WT_{\ O\ \&\ M,}}$ and $\mathrm{WT_{REP}}$, respectively. Capital costs include costs for wind turbines, structural costs, and other components. Labor costs, transportation, and installation costs are included. Annual costs of operating and maintenance where the project time in years is displayed by T lifetime. Replacement expenses comprise any protective or other element that must be replaced after a certain period, whereas N_{REP} constitutes the number of components that must be replaced over the whole life of the project.

4.3 Hydro

A 15 kW microhydro turbine of Generac is used in the study with an efficiency of 75%. The available electricity is critical to the reservoir plant's operation. This may be concluded from the observation that Eq. 10 calculates the potential power of a mass m of water at h (Majdi Nasab et al., 2021).

$$E = mgh \tag{10}$$

where g denotes gravity's acceleration. There are friction losses in the penstock, as well as losses in the turbine. This impact is taken into account using a multiplication factor, and the electric power available from a turbine with head h is given by.

$$P = \eta \rho Q g h \tag{11}$$

The flow rate of the hydro turbine is the intermediate variable of the microturbine output power. Using the criteria stated below, the output power of a microhydro may be calculated at various time stages.

$$P_{\mathrm{turbine}} = \begin{cases} 0 & if\ Q_{\mathrm{available}} < Q_{\mathrm{min}} \\ P_{\mathrm{available}} & if\ Q_{\mathrm{min}} \le Q_{\mathrm{available}} \le Q_{\mathrm{max}} \\ P_{\mathrm{max}} & \mathrm{if}\ Q_{\mathrm{max}} \le Q_{\mathrm{available}} \end{cases} \tag{12}$$

Equation (13) is given for the cost analysis of the microhydro system.

$$\mathrm{MH_{NPC}} = \mathrm{MH_{CC}} + \mathrm{MH_{ins}} + \sum_{1}^{n} \mathrm{MH}_{O\&M} * T_{lifeTime} + \mathrm{MH_{rep}} * N_{\mathrm{rep}} \tag{13}$$

where $\mathrm{MH_{NPC}}$, $\mathrm{MH_{CC}}$, $\mathrm{MH_{ins}}$, $\mathrm{MH_{O\&M}}$, and MHrep are net costs of installation, cost of capital, costs for operations and maintenance, and cost of replacement accordingly of a microhydro system. Capital costs include turbine costs, generator costs, and equipment protection costs. Includes wage costs, civil works, transportation, and installation costs for the installation. Annual operational and maintenance expenditures for the microhydroelectric system, where lifetime denotes the project's life in years. Replacement expenditures include any protective or other part that must be replaced after a given time, where Nrep represents the number of components that must be replaced during the project's whole life.

4.4 Diesel generator

The system design and simulation processes used a Genset small-size diesel generator. The minimum load ratio of 25% is considered which estimates a life span of 15,000 h (Rezk et al., 2020) and a fuel price of $ 0.80 per liter. Equation (14) shows the power output from a diesel generator (Falama et al., 2022) while Eq. (15) can be used to calculate the CO_2 emission (Shezan et al., 2022)

$$P_G = n_{\mathrm{diesel}} * \mathrm{NDG} * \mathrm{PGD}, N \tag{14}$$

$$\mathrm{CO_2} = 3.667 * m_f * \mathrm{Hv}_f * \mathrm{CEF}_f * x_c \tag{15}$$

where NDG = total number of identical diesel generators, PDG = combined output power of the generators, n is the efficiency of the generator, $\mathrm{m_f}$ is the total amount of fuel, while $\mathrm{Hv_f}$, $\mathrm{CEF_f}$, and X_c present tons of carbon emitted per TJ, the percentage of oxidized carbon, and heating value of fuel in MJ/L, respectively. 3.66 is the constant of carbon in CO_2.

4.5 Converter cost function

The HOMER built-in power converter is used in this study. The converter has an efficiency of about 90%. It works in both the inverter (Inv) and rectifier (Rec) modes. When the battery is being charged it acts as the rectifier, while when power is being supplied to the load from PV/battery it acts as an inverter. The cost function of a converter is depicted in Eq. (18) (Prakash & Dhal, 2021).

$$\mathrm{CON_{NPC}} = \mathrm{CON_{CC}} + \mathrm{CON_{ins}} + \mathrm{CON}_{O\&M} * T_{\mathrm{lifeTime}} + \mathrm{CON_{rep}} * N_{\mathrm{rep}} \tag{18}$$

The net present costs, capital costs, installation, operating and maintenance costs as well as substitute costs of solar conversion are present in $\mathrm{CON_{NPC}}$, $\mathrm{CON_{CC}}$, CONins, $\mathrm{CON_{O\&M,}}$ CONrep, and CONrep. Capital costs include converter costs, interrupters, Ethernet boxes, etc. Capital costs. The cost of installation includes costs of labor, shipping, and assembly. Annual operating and maintenance cost where lifetime displays project life in years. Replacement costs include any units that must be replaced after a certain period, whereas Nrep represents the number of components that must be replaced throughout the project.

4.6 Battery bank

The battery used in the study is a 20 kilowatt-72 kilowatt-hour Primus energy cell. It is a zinc–bromine battery. The battery bank is used as a backup system. Roundtrip efficiency is about 72 percent while the maximum charge current is about 250 amperes, and the maximum discharge current is considered 500 amperes. It has a nominal voltage of 60 V. It stores energy when the system is over producing and then provides it when the system is under producing. Equation (19) shows the cost function of battery bank (Omotoso et al., 2022).

$$\mathrm{BB_{NPC}} = \mathrm{BB_{CC}} + \mathrm{BB_{ins}} + \sum_{1}^{n} \mathrm{BB}_{O\&M} * T_{\mathrm{lifeTime}} + \sum_{1}^{n} \mathrm{BB_{rep}} * N_{\mathrm{rep}} - P_{\mathrm{salvage}} \quad (19)$$

$\mathrm{BB_{NPC}}$, $\mathrm{BB_{CC}}$, BBins, $\mathrm{BB_{O\&M}}$, and $\mathrm{BB_{REP}}$ are the actual costs of the battery bank, net present, capital, installation, and operation and maintenance costs, respectively. Battery purchases, battery bank racks, connectors, and other supplies will be included in the capital cost. Labor, delivery, and assembly are all included in the installation fee. The lifetime represents project life for years while operating and servicing expenses in one battery per year. The expenses of replacement include the number of batteries that must be replaced after their life cycle is complete, with the Nrep battery needing to be replaced numerous times during the project. $\mathrm{P_{salvage}}$ is the cost at the end of the project life of these batteries.

4.7 Economics of the project

The core variables of the economics are the nominal discount rate (NDR) is fixed at 10%, while the presumed inflation rate is fixed at 2%, and the 25 years of the project's lifetime.

4.8 System dispatch strategies

For the analysis of dispatch strategies in this study, two strategies were considered: cycle charging (CC) and load following (LF). The HOMER software was utilized to evaluate and determine the most suitable strategy for each system configuration.

In the load following strategy, the power generation is adjusted to precisely meet the system's demand. Only the required amount of power is generated to satisfy the load at any given time. On the other hand, the cycle charging strategy involves operating the diesel generators at their full capacity to fulfill the load requirements, while any excess energy generated is used to charge the available battery banks (Adil Khan et al., 2019; Zameer & Wang, 2018).

Furthermore, the configurations in the study allow for the simultaneous operation of multiple generators. An operating reserve of 10% of the hourly load is maintained to account for unexpected variations in load. For solar and wind systems, the operating reserve values are set at 100% and 80%, respectively. The operating reserve serves as additional operating capacity that can be utilized in case of unforeseen fluctuations in load or renewable energy generation. Its purpose is to ensure the uninterrupted supply of electricity to the system.

By considering both the CC and LF dispatch strategies and incorporating an operating reserve, the hybrid energy systems can effectively manage fluctuations in demand and renewable energy generation, thereby ensuring a reliable and uninterrupted power supply.

4.9 Sensitivity variable

To assess the influence of individual variables on the overall system design, a sensitivity analysis was conducted. This analysis aims to examine the impact of changes in specific variables, such as fuel price, equipment cost, wind speed, and other relevant factors. Since these variables are subject to fluctuations due to technical and environmental considerations, it is crucial to evaluate the system's robustness through sensitivity analysis.

During the sensitivity analysis, a range of variables was taken into account to determine the optimal design of the hybrid system that can effectively meet the load demand sustainably. The variables considered for the sensitivity analysis are presented in Table 3. Each variable was carefully examined to assess its effect on the system, and a detailed analysis was conducted to understand the implications of variations in these variables. By conducting this sensitivity analysis, we gain valuable insights into the system's performance and its ability to adapt to changing conditions, ensuring its reliability and sustainability.

5 Results and discussion

To find the most effective, reliable, and sustainable system HOMER software was used. Eight different systems were designed in the software using different combinations from sources that included diesel generator, PV, wind, hydro, and batteries. All of them were compared based on output power, NPC, LCOE, and CO_2 emissions. MCDA was used to identify the best system based on the defined parameters.

5.1 Component specification of the hybrid systems

The technical specifications of the PV module, hydro turbine, wind turbine, diesel generator, converter, and batteries that were used in the different systems in HOMOR PRO are presented in Table 4, 5, 6. Table 4 shows the component specifications of systems 1–4. System 1 was a stand-alone generator system while the rest three were hybrid generators with individual renewable energy sources of hydro, PV, and wind, respectively. Diesel is used as fuel for the generator. Similarly, Table 5 shows the component specification of systems 5–8 which are hybrid systems of renewable sources only. Table 5

Table 3 Sensitivity variables for analysis

Sensitivity variables	Unit	Values
Capacity shortage	(%)	0%, 1%
Diesel fuel price (DFP)	($/l)	0.8, 1
Load growth	(kWh/day)	428, 535
Nominal discounted rate	(%)	8, 10
Project lifetime	(years)	15, 25
Expected inflation rate	(%)	2, 4

Table 4 Component specification of the hybrid system 1–4

Quantity	Units	System 1 Generator	System 2 Generator	System 3 Generator	System 4 Generator
		Value	Value	Value	Value
Operational hours	hrs/yr	8760	2456	7760	6915
Number of starts	starts/yr	1.00	490	1.00	533
Operational lifetime	year	2.85	10.2	3.15	3.62
Capacity factor	%	42.2	7.49	33.3	25.5
Fixed generation cost	$/hr	1.56	1.56	1.56	1.56
Marginal generation cost	$/KWh	0.197	0.197	0.197	0.197
Electrical production	KWh/yr	92,360	16,405	72,931	55,930
Min electrical output	KW	6.25	6.25	6.25	6.25
Max electrical output	KW	21.8	13.4	20.9	21.8
Fuel consumption	L	32,441	6,505	27,137	20,974
Specific fuel consumption	L/KWh	0.351	0.397	0.372	0.375
Fuel energy input	KWh/yr	319,222	64,008	267,028	206,381
Mean electrical efficiency	%	28.9	25.6	27.3	27.1
			Hydro	PV	Wind
Rated capacity	KW	–	15.0	18.6	10
Minimum output	KW	–	10	3.70	3.05
Capacity factor	%	–	91.4	19.9	30.5
Total production	Kwh/yr	–	102,151	32,439	26,688
Maximum output	KW	–	13.7	15	7
Source penetration	%	–	133	36.0	29.6
Operation hours	Hrs/yr	–	8016	4384	8175

presents the specifications of the renewable sources while Table 6 shows the specifications of the converter and batteries used in them.

Table 4 shows that system 1 relies solely on a diesel generator and operates continuously for 8760 h annually. The single start indicates that it supplies power uninterrupted to the region. However, due to the continuous operation, system 1 has the lowest operational lifetime among all the hybrid systems along with maximum fuel consumption. With the addition of renewable sources to the hybrid system (systems 2–4), the load is shared between the two sources. This decreases the sole dependency on the generator. The generator's operational hours reduce which increases the generator's operational lifetime. The electric production of the generator also reduces which is compensated by the renewable energy power sources. This causes less diesel fuel consumption which reduces running costs and GHG emissions of the generator. As the source of fuel varies for each renewable system, they contribute in different proportions in their respective systems which are presented in Table 4. System 2 combines a diesel generator with hydropower. The hydro turbine has a rated capacity of 15kw which provides 90% of the power, producing 102,151kWh/year, drastically reducing the generator operation. In this system, the generator acts as a backup source as indicated by the high number of starts

Table 5 Component specification of the hybrid system 5–8

Quantity	Units	System 5	System 6	System 7	System 8	
		Wind	Solar	Solar	Solar	Wind
		Value	Value	Value	Value	Value
Rated capacity	KW	50	84	103	31.3	20.0
Minimum output	KW	15.2	16.7	20.6	6.24	5.99
Capacity factor	%	30.0	19.9	19.9	28	30.5
Total production	Kwh/yr	31,188	146,585	180,246	54,700	52,475
Maximum output	KW	48	80	100	19.9	18
Source penetration	%	146	163	200%	60.7	58.2
Operation hour	Hrs/yr	8,175	4,284	4,284	4,384	8,175

		Hydro	Hydro	Wind	Hydro
Rated capacity	KW	15.0	15.0	40.0	15.0
Minimum output	KW	10	10	12.0	10
Capacity factor	%	91.4	91.4	30.0	91.4
Total production	Kwh/yr	120,151	120,151	104,950	120,151
Maximum output	KW	13.7	13.7	38	13.7
Source penetration	%	133	133	116	133
Operation hours	Hrs/yr	8016	8016	8175	8016

(490) while hydro is the main supplier. The hydro source has an operational time of 8,016 h/year while the generator has 2,456 h/year.

In system 3 (generator + PV), the majority chunk of the load again falls on the diesel generator with it producing 70% of the power and the PV producing 30%. The single start indicates that the generator runs continuously reducing the generator's lifetime and increasing fuel cost. An 18.6kW PV source is used in the system which acts as a supplementary source. The PV source has a production and operation time of 32,439kWh/year and 4,384 h/year. Similarly, in system 4, the generator still provides about 65% of the power, but the higher number of starts (533) indicates that it does not provide continuous power but operates in durations. The discontinuous operation increases the operation lifetime of the system and reduces cost as compared to system 1 and 3. In the periods where the generator is off the power is supplied by the wind turbine system of 10 kW.

Systems 5–8 are fully renewable hybrid systems that combine various combinations of wind, solar, and hydro energy sources. Table 5 shows that in each system different combinations are used which causes contrasting values for each parameter such as rated capacity, total power production, and operation time. In system 5, the hydro source of 15kW has a high capacity factor of 91.4%, indicating that it provides power as a consistent and reliable supply. The total energy production from hydro is a significant 120,151 kWh/year while the wind turbine produces 31,188 kWh/year. Given its higher capacity factor and energy output, the hydro is the primary source while the wind is the secondary. Similar to system 5, in system 6 hydro is the main source while the PV system is the secondary source. The hydro has a capacity factor of 91.4%, producing 120,151 kWh/year while the PV source produces 146,585 kWh/year with a capacity factor of 19.9%. System 7 is a hybrid of PV and wind source. With a rated capacity of 103 kW and a capacity factor of 19.9%, the solar component produces 180,246 kWh/year, operating for 4,284 h. The wind component in

Table 6 Component specification of the hybrid system 5–8

Quantity	Units	System 5 Batteries	System 6 Batteries	System 7 Batteries	System 8 Batteries
		Value	Value	Value	Value
Batteries	qty	356	564	416	312
String size	batteries	4.00	4.00	4.00	4.00
Strings in Parallel	strings	89.0	141	104	76.0
Bus voltage	V	48.0	48.0	48.0	48.0
Autonomy	hr	17.3	27.4	20.2	14.8
Storage Wear Cost	$/KWh	9.53	9.53	9.53	9.53
Nominal capacity	KWh	356	564	416	304
Usable nominal capacity	KWh	178	282	208	152
Lifetime Throughput	KWh	34,076	62,676	286,830	32,677
Expected life	yr	12.0	12.0	12.0	12.0
Energy In	KWh/yr	3,174	5,839	26,718	3,044
Energy Out	KWh/yr	2,539	4,672	21,379	2,436
Losses	KWh/yr	635	1,168	5.60	609
Annual Throughput	KWh/yr	2,839	5,223	5,344	2,723

		Converter (System 5)		Converter (System 6)		Converter (System 7)		Converter (System 8)	
		Inv	Rec	Inv	Rec	Inv	Rec	Inv	Rec
Capacity	KW	36.6	36.6	18.9	18.9	25.9	25.9	15.6	15.6
Minimum Output	KW	0.275	0.362	1.21	0.254	4.45	0.400	0.466	0.174
Maximum Output	KW	13.2	36.6	13.4	9.61	21.8	25.9	13.4	13.8
Capacity Factor	%	0.75	0.99	6.39	1.34	17.2	1.54	2.99	1.1
Operation Hours	hrs/yr	748	8008	2332	1105	5254	1703	1204	3838
Energy Out	KWh/yr	2412	3174	10,601	2225	39,009	3501	4083	1522
Energy In	KWh/yr	2539	3341	11,159	2342	41,062	3685	4298	1602
Losses	KWh/yr	127	167	558	117	2068	184	215	80.1

system 7 has a rated capacity of 40 kW and a capacity factor of 30%, producing 104,950 kWh/yr. This indicates a balanced contribution from both solar and wind sources, making this system versatile and adaptive to varying renewable energy availabilities. System 8 is a hybrid of all three renewable sources. Similar to the previous systems, the hydro component remains consistent with a capacity factor of 91.4% and an energy production of 120,151 kWh/year. It acts as the backbone of the system, ensuring a consistent energy supply. In periods when hydro production is low, it is complimented by the PV and wind source. The PV component in system 8 has a rated capacity of 31.3 KW, with a capacity factor of 28%, and produces energy of 54,700 kWh/year for 4,384 h annually. The wind energy component has a capacity of 20 kW, with a capacity factor of 30.5%, producing 52,475 kWh/year over 8,175 h. The wind component, though lesser in capacity than solar, provides consistent energy output, ensuring the system's stability.

Each renewable energy source contributes differently in each system which has led to different sizing and rating of the battery bank and converter in each system as shown in Table 6. System 5, which is designed to backup wind and hydropower, consists of 196 batteries grouped in 4 parallel strings, ensuring a reliable energy reservoir with a bus voltage of 48 V and a 17.3-h autonomy. These batteries have a nominal capacity of 356 kWh, and with an expected lifespan of 12 years, they promise long-term reliability. Complementing this, the converter system, with both an inverter and a rectifier rated at 36.6 kW, ensures efficient energy conversion. The inverter converts 2412 kWh/year, while the rectifier outputs 3174 kWh/year. This balanced conversion ensures optimal utilization of stored energy, making system 5 a robust backup for the wind and hydro hybrid. System 6, tailored for solar and hydro energy, employs 280 batteries arranged in 4 parallel strings. These batteries provide an autonomy of 27.4 h with a nominal capacity of 564 kWh. The converter is rated at 18.9 kW. The inverter converts 10,601 kWh/year, whereas the rectifier contributes 2225 kWh/year. For system 7, backing up solar and wind energy, the design incorporates 208 batteries in 4 parallel strings. They guarantee an autonomy of 20.2 h and a nominal capacity of 416 kWh. The converter of 25.9 KW manages energy conversion adeptly. The inverter contributes 39,009 kWh/year, while the rectifier contributes 3501 kWh/year. Similarly, system 8, an advanced backup for solar, wind, and hydro energy, integrates 312 batteries organized in 4 parallel strings. These batteries offer an autonomy of 14.8 h and a nominal capacity of 304 kWh. The converter system, vital for energy transition, consists of a 15.6 KW inverter and rectifier. The inverter yields 4083 kWh/year, and the rectifier outputs 1522 kWh/year.

5.2 Cost analysis

The comprehensive cost analysis for the eight hybrid systems, as presented in Table 7, encompasses various financial aspects, including the capital cost, replacement cost, operations and maintenance (O&M) cost, fuel cost, and salvage value. Each system's total net present value, a critical financial metric, is derived from these individual costs.

Distinct combinations of energy systems result in varied technical specifications, thereby influencing the associated costs of each hybrid system. For instance, system 7 demands the highest capital investment, amounting to $133,440.26, due to its larger rated capacity. In stark contrast, system 1 is the most economical in terms of initial capital outlay, requiring only $24,101.46.

Table 7 Cost analysis of the hybrid systems 1–8

	Capital ($)	Replacement ($)	O & M ($)	Fuel ($)	Salvage ($)	Total net present
System 1	24,101.46	99,139.47	471.85	302,889.55	1385.69	425,216.64
System 2	31,879.23	20,997.73	7314.25	60,732.71	3140.89	117,783.06
System 3	30,405.95	99,139.47	15,919.71	253,365.98	1385.69	397,445.44
System 4	79,657.01	74,607.68	29,100.29	195,821.89	4900.76	378,690.61
System 5	122,680.97	26,959.37	70,236.66	–	7817.57	212,059.43
System 6	97,215.80	42,710.92	115,544.29	–	12,385.14	243,085.87
System 7	133,440.26	31,503.09	142,157.49	–	9135.14	297,965.70
System 8	80,759.54	23,018.71	69,068.43	–	6675.68	166,173.78

However, the fuel cost dynamics offer a different perspective. System 1, being entirely reliant on a diesel generator, incurs a substantial fuel expense of $302,889.55, the highest among all systems. This high cost underscores the financial implications of relying heavily on non-renewable energy sources. Conversely, systems 5 to 8, with their renewable energy compositions, eliminate the need for conventional fuels, resulting in zero fuel costs.

Replacement costs vary across systems, with system 8 demonstrating frugality at $23,018.71, while system 1 necessitates a considerable $99,139.47, due to the wear and tear of the generator components. O&M costs offer another dimension to consider. System 7 has the steepest O&M expenses at $142,157.49, hinting at the intensive maintenance needs of its components. System 1, despite its high fuel cost, manages to keep its O&M expenses minimal at $471.85.

Salvage value, representing the estimated value of an asset at the end of its useful life, varies across the systems. System 6 stands out with the highest salvage value of $12,385.14, suggesting a higher residual value of its components. In contrast, system 1's components depreciated significantly, leaving a salvage value of only $1,385.69.

Taking all these cost components into account, the total net present value provides an overarching financial perspective. System 1, with a value of $425,216.64, emerges as the most expensive in its lifecycle, largely driven by its fuel costs. On the other hand, system 8 proves to be the most cost-effective option with a total net present value of $166,173.78, underscoring its economic and sustainable design. In terms of financial cost analysis (Lajunen, 2014), system 8 is the best option.

5.3 Hybrid system performance

Figure 11 illustrates the levelized cost of energy (LCOE) across all hybrid systems, a pivotal metric in gauging the cost-effectiveness of energy systems over their operational lifespan. System 1, operating solely on a diesel generator, inherently relies on a continuous supply of diesel. Diesel, being a non-renewable resource, comes with market-driven price fluctuations and availability concerns. This constant dependency on fuel, combined with the environmental and logistical costs associated with diesel procurement, storage, and consumption, inevitably escalates its LCOE, making it the highest among all systems. As we transition to systems 2 through 4, the incorporation of renewable energy sources starts to change the LCOE dynamics. Renewable sources, once installed,

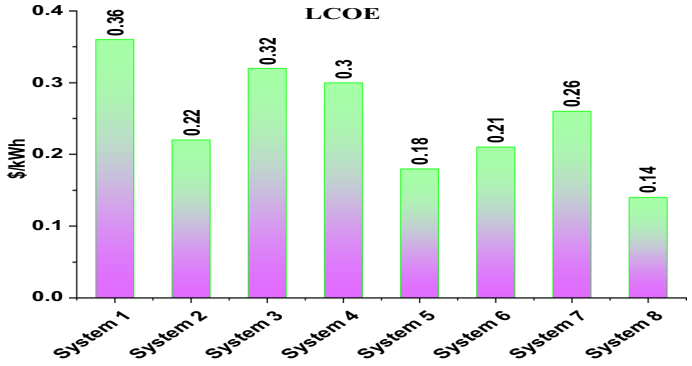

Fig. 11 LCOE of the different hybrid systems

have minimal marginal costs, especially when it comes to fuel. They harness energy from natural sources like sunlight, wind, and water flows, which are not only abundant but also free. Thus, as these renewable sources begin to contribute more to the power production responsibility, the diesel generator's operational hours reduce. This reduction translates directly into decreased fuel consumption and, by extension, a declining LCOE.

Systems 5 to 8 represent a major shift. Completely removing the diesel generator, they rely purely on renewable energy combinations. The absence of any fuel costs for these systems is a game changer. With zero diesel consumption, the LCOE is influenced by capital, operations, and maintenance costs—all of which tend to be competitive in the long run, especially when considering the environmental externalities.

Among these, system 8 stands out. It harnesses the power from three renewable sources: photovoltaic (PV) panels, wind turbines, and hydro energy. This trio ensures diversified energy input, minimizing the vulnerabilities associated with any single renewable source's intermittent nature. The system benefits from the consistent energy supply of hydro, the daytime efficiency of PV, and the often complementary generation patterns of wind (Lajunen, 2014).

Greenhouse gas (GHG) emissions remain at the forefront of global environmental concerns, primarily due to their unequivocal association with climate change. Figure 12 shows the environmental footprints of the different hybrid systems based on their energy source. Systems 1 through 4 incorporate a diesel generator, inherently leading to high GHG emissions during operation. The combustion process within the generator produces carbon dioxide (CO_2), nitrogen oxides (NOx), and other GHGs, linking the system's operational hours directly with its emissions. System 1, being exclusively reliant on its diesel generator for power generation, inevitably records the highest GHG emissions. The continuous combustion of diesel not only results in significant carbon emissions but also other pollutants that have both environmental and health implications.

However, a transformation is observed in systems 2, 3, and 4. The integration of renewable energy sources in these systems introduces a shift. As these green energy

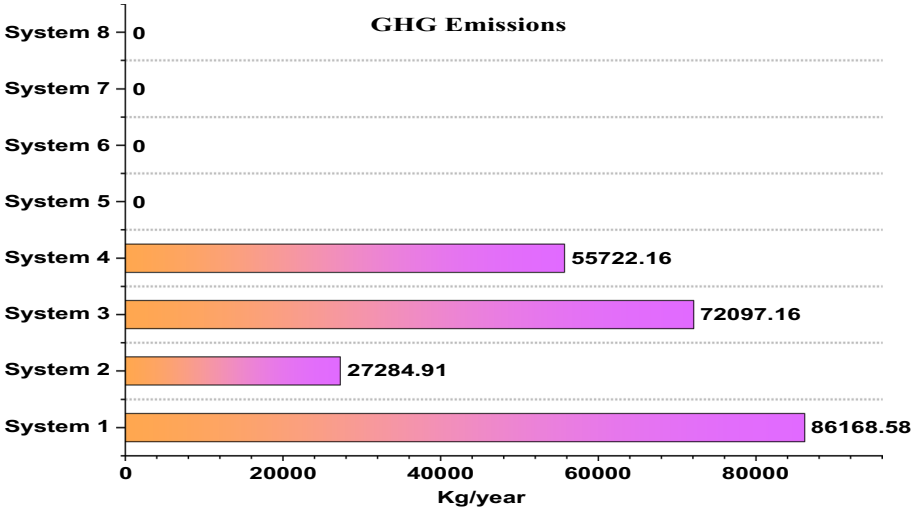

Fig. 12 GHG emissions of all the hybrid system

sources begin to contribute to the energy mix, they offset the generator's operational load. The direct consequence is a decline in diesel consumption, leading to proportionally reduced GHG emissions (Lajunen, 2014). Specifically, the hydro-based component in system 2 demonstrates remarkable efficacy in reducing emissions, making it the most environmentally friendly among the first four systems.

On the other end of the spectrum lie systems 5 through 8, embodying the pinnacle of sustainable green energy generation. Operating purely on renewable sources, these systems achieve the gold standard in environmental performance of zero GHG emissions. Their operation remains entirely decoupled from any combustion processes, ensuring that their energy generation does not contribute to the global GHG inventory.

GHG emissions are not monolithic. They encompass a diverse array of gases, each with its unique molecular structure, radiative properties, and environmental impact. Central among these is carbon dioxide (CO_2), the largest product of burning fossil fuels. However, GHG emissions also include other deleterious compounds such as carbon monoxide (CO), nitrogen oxides (NO), sulfur dioxide (SO_2), unburnt hydrocarbons, and particulate matter. Each of these compounds, while differing in their relative abundances, plays a role in atmospheric processes, affecting air quality, human health, and the broader environment. Particularly, their cumulative effect has been linked to the degradation of the ozone layer and the exacerbation of global warming, as substantiated by numerous scientific studies (Bakır et al., 2022). Figure 13 shows the different gas compositions in the GHG emissions of systems 1–4.

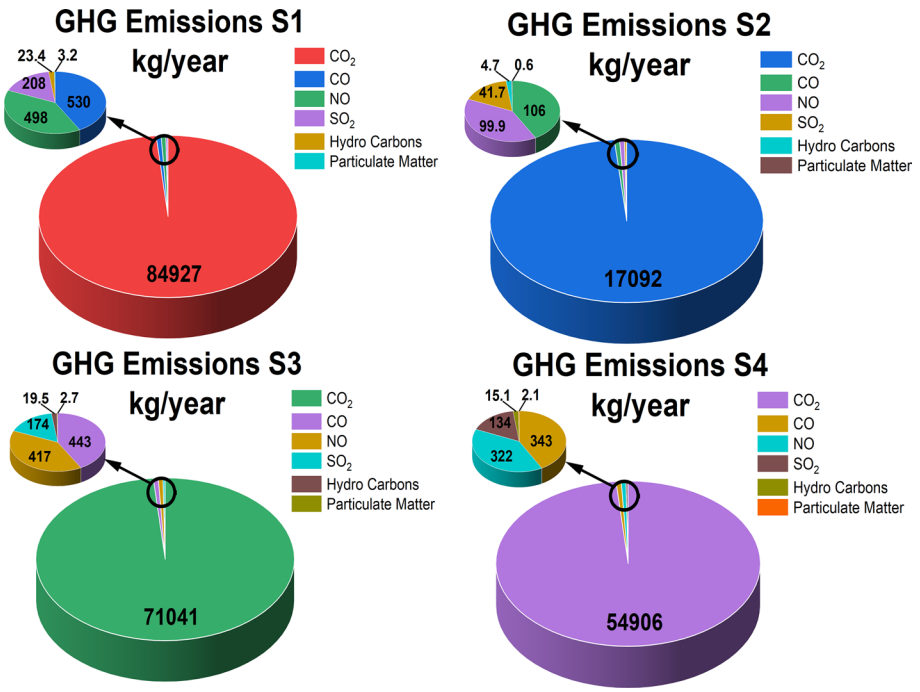

Fig. 13 GHG emission composition

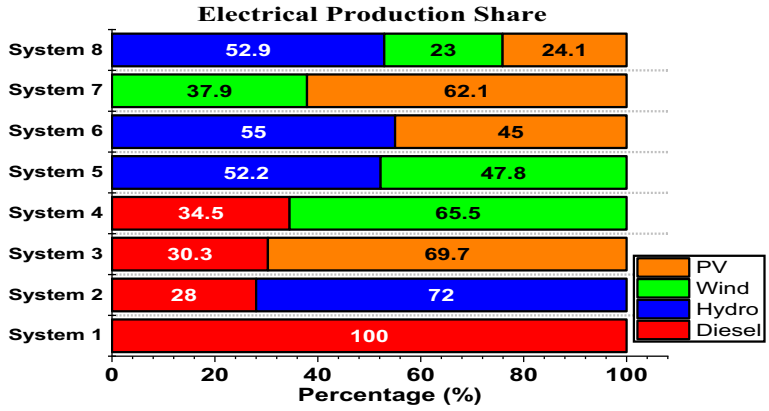

Fig. 14 Energy sources' contribution to electrical production

The eight hybrid systems are made of different energy sources which include diesel, solar, wind, and hydro. The sources contribute differently to each system. The contribution depends on the availability of the source which greatly depends on the climate and geographical conditions. Figure 14 shows the percentage of contribution of each source in every system. Due to the geographical location, there is an almost constant supply of hydro energy with dry spells only in January. Because of this reason in all the systems where hydro is used, it contributes more than 50% of power production. The location also has excellent spells of solar and wind availability; therefore, it can be seen that they also contribute to power production.

In systems 5 and 6, they contribute more than 40%, respectively, along with hydro in power production. Solar has a slightly more share than wind in the location's energy mix as can be seen from the results of system 8 and system 7 (more than 60% is contributed by solar). It can also be seen that as renewable energy sources are introduced in systems 2, 3, and 4, the generator contribution reduces significantly below 35%.

Figure 15 offers a comprehensive visualization of the daily and hourly electrical output for each energy source in the hybrid systems throughout the year. A discernible pattern emerges, particularly influenced by the diurnal rhythms and the varying load demands. It's evident that during nighttime when the load is minimal, the output from the sources diminishes. This reduction is particularly pronounced for sources that rely on daylight, such as solar. Conversely, daytime, especially during summer months, witnesses a surge in energy production. This escalation can be attributed to increased load demands, often reaching peak levels due to heightened commercial and residential activities.

The intermittent nature of renewable energy sources is also evident. Periods or "dry spells" occur during which specific sources, owing to environmental factors, produce little to no power. However, the hybrid design of the systems ensures that when one source is underperforming, other steps in to compensate, guaranteeing an uninterrupted power supply. A case in point is system 2. Here, the hydro system experienced a dry spell in January, resulting in no power generation. Yet, the diesel generator compensates for this deficit, especially during peak load periods. At other times, its contribution is negligible, underscoring the system's reliance on hydropower.

System 8 provides a more intricate output pattern. In the absence of hydropower in January, the wind turbine plays a pivotal role. Yet, throughout the year, peak hour demands

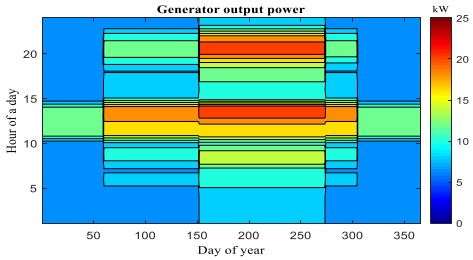

a. System-1 energy sources power-output

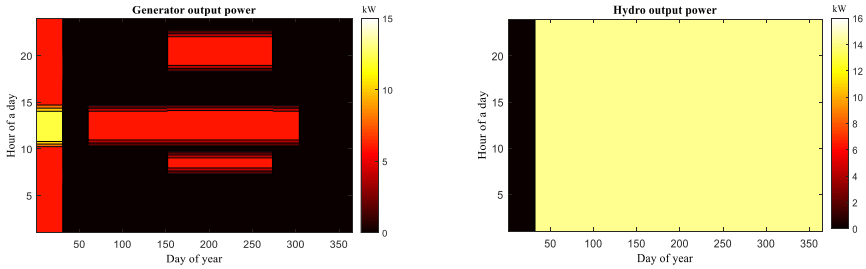

b. System-2 energy sources power-output

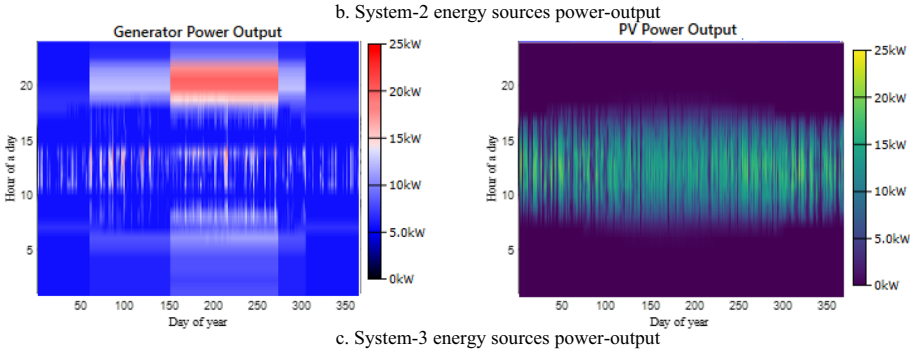

c. System-3 energy sources power-output

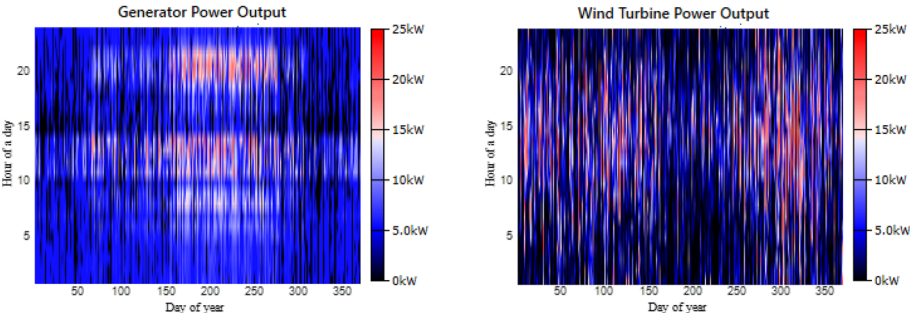

d. System-4 energy sources power-output

Fig. 15 **a** System 1 energy sources power output, b system 2 energy sources power output, **c** system 3 energy sources power output, **d** system 4 energy sources power output, **e** system 5 energy sources power output, **f** system 6 energy sources power output, **g** system 7 energy sources power output, **h** system 8 energy sources power output

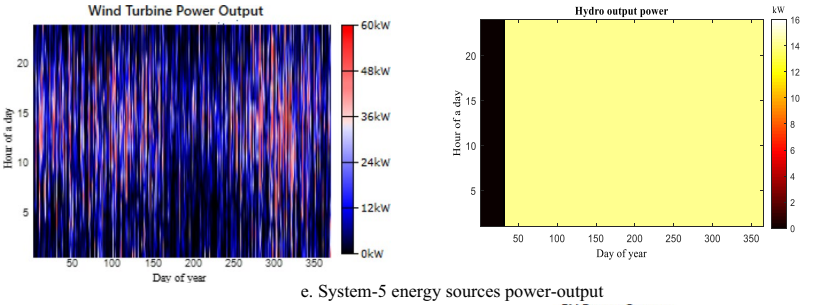

e. System-5 energy sources power-output

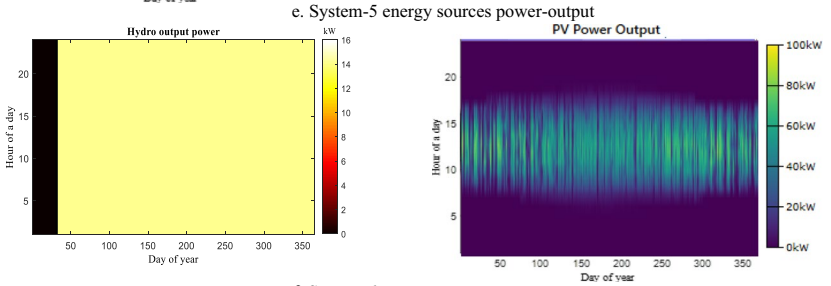

f. System-6 energy sources power-output

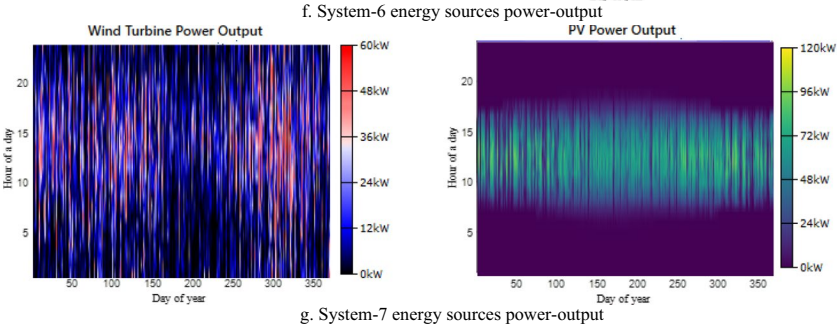

g. System-7 energy sources power-output

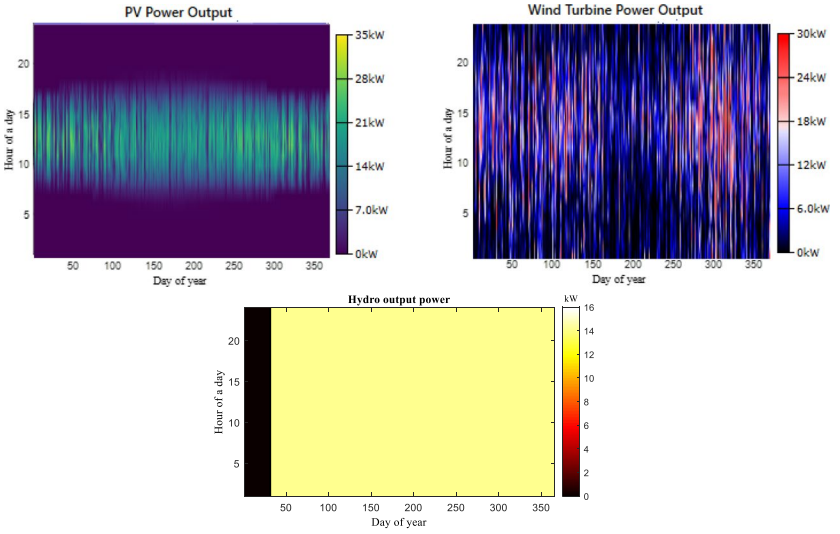

h. System-8 energy sources power-output

Fig. 15 (continued)

are predominantly met by the combined efforts of the microhydro and solar PV. However, during winter months, when solar output wanes due to reduced daylight hours, the wind turbines, in conjunction with batteries, ensure that the system caters to the elevated residential loads.

Across all systems, a recurring theme is evident. Each energy source, with its unique operational characteristics, complements the others. Periods of reduced output from one source are effectively counterbalanced by increased production from another. This harmony ensures that irrespective of environmental variables or load demands, a consistent power supply is maintained. Figure 15, in essence, underscores the resilience and adaptability of the hybrid systems, showcasing how diverse energy sources can seamlessly integrate to ensure stable power.

5.4 Breakeven Grid Extension Distance (BGED)

The breakeven grid extension distance (BGED) serves as a metric to assess the cost-effectiveness of implementing a stand-alone energy system versus extending the grid to a specific location. It compares the distance between the location and the grid station with the BGED value to determine the most economical option (Table 8).

For the system 8 configuration in the Bankhwar Utrar region, the calculated BGED is 75.75 km. This value is considerably lower than the actual distance of 112 km between Bankhwar Utrar and the alternate district grid at Kalam. Hence, based on the BGED of 75.75 km, it is evident that constructing a stand-alone system would be more cost-effective than extending the grid to the alternate grid. This implies that investing in a stand-alone system is a favorable and economically viable choice for meeting the energy needs of the Bankhwar Utrar community.

6 Multi-criteria decision-making (MCDM)

The HOMER Pro software optimizes the system by prioritizing the lowest net present cost (NPC) and cost of electricity (COE) while ensuring the load demands are satisfied. However, it does not take into account other crucial parameters of the system. To address this limitation, the multi-criteria decision-making (MCDM) method was employed to rank the systems, considering the inclusion of other significant factors.

Table 8 BGED of the hybrid energy systems

System	BGED (km)
System 8	75.75
System 2	102
System 5	115.65
System 6	147.17
System 7	157.67
System 4	186.36
System 3	204.69
System 1	237.54

MCDM is a decision-making approach that involves the assessment of multiple solutions based on predetermined criteria and common challenges. In this study, the criteria were assigned weights using the analytical hierarchy process (AHP) technique, which allows for the relative importance of each criterion to be determined. Subsequently, the simple additive weightage (SAW) method was utilized for data analysis and evaluation. The SAW method, also referred to as the weighted summing method, calculates the weighted sum of performance evaluations for each alternative across all attributes.

The criteria identified for the MCDM method are shown in Table 9. The criteria were selected based on the output results obtained from HOMER Pro and then identified their relative importance by carrying out an extensive literature review.

To account for the varying levels of importance attributed to the evaluation criteria, a rigorous selection process was employed in this study. The chosen criteria were specifically customized to suit the unique circumstances that could potentially impact the performance of the installed renewable energy systems. To determine the appropriate weighting for each criterion, the analytic hierarchy process (AHP) method was employed. To facilitate this procedure, a comparison decision matrix was constructed, enabling direct evaluations between each criterion and its corresponding counterpart. This approach facilitated the identification of the most significant criteria, ensuring a comprehensive and systematic evaluation of the renewable energy systems under investigation.

The pairwise comparison matrix employed a scale ranging from 1 to 9, signifying the relative importance of each criterion. It was created using a square matrix $A = m * m$, where "m" represents the number of criteria. The entries in the comparison matrix, denoted as a_{ij},

Table 9 Selected criteria for MCDM

Criteria	Symbol	
Renewable energy penetration	C1	Beneficial
Excess power	C2	Beneficial
Unmet load	C3	Non-beneficial
Breakeven grid extension Distance (BGED)	C4	Beneficial
Levelized cost of electricity	C5	Beneficial
Net present cost	C6	Non-beneficial
O&M	C7	Non-beneficial
GHG emissions produced	C8	Non-beneficial

Table 10 Pairwise values of comparison matrix

	C1	C2	C3	C4	C5	C6	C7	C8
C1	1	0.33	4	3	0.17	0.14	2	2
C2	3	1	2	2	0.17	0.14	0.5	1
C3	0.25	0.5	1	2	0.2	0.17	0.5	0.5
C4	0.33	0.5	0.5	1	0.2	0.2	0.5	2
C5	6	6	5	5	1	0.5	4	6
C6	7	7	6	5	2	1	5	6
C7	0.5	2	2	2	0.25	0.2	1	2
C8	0.5	1	2	0.5	0.17	0.17	0.5	1

represented the comparison values between the *i*th (row) criterion and the *j*th (column) criterion. The values for the comparison matrix, as presented in Table 10, were established through Eq. 20, enabling direct evaluations between each criterion and its corresponding counterpart. These values in Table 10 were derived through an extensive literature review, encompassing multiple articles on MCDM applied in the context of renewable energy. A thorough analysis of these articles allowed for the identification of the relative importance of each criterion and the assignment of corresponding numerical values.

Furthermore, a priority vector was generated for the matrix and subsequently verified through the consistency verification process. The resulting consistency ratio (CR) was found to be below 10% (8.9%), providing validation for the matrix's reliability in the decision-making process. This meticulous approach ensures the robustness and accuracy of the evaluation process, facilitating informed decision-making regarding the renewable energy systems being assessed.

$$A = \left(a_{ij}\right) \tag{20}$$

$$a_{ij} = \frac{1}{a_{ji}} \quad if\ i \neq j$$

$$else\ if\ i = j,\ a_{ij} = 1$$

In the next phase, to ensure consistency and comparability, each entry value (a_{ij}) in the pairwise comparison matrix needs to be normalized. This normalization is achieved by dividing each entry value by the sum of the entry values within its respective column. The purpose of this process is to create a normalized pairwise comparison matrix where the values accurately reflect the relative importance of the criteria being evaluated. The calculation of the normalized matrix is determined by utilizing Eq. 21, which ensures that the resulting values maintain their proportional significance in the decision-making process.

$$a_{ij} = \frac{a_{ij}}{\sum_{l=1}^{m} a_{lj}} \tag{21}$$

To derive the overall weight vector, the final step entails calculating the average of each row in the matrix provided in Table 11. This averaging procedure is performed using Eq. 22, which ensures that the resulting weights reflect the collective importance assigned to the criteria. By averaging the values within each row, we obtain a comprehensive representation of the relative significance of the criteria in the decision-making process.

$$w_i = \sum_{l=1}^{m} a_{il} \tag{22}$$

The multi-criteria utility function (U) plays a vital role in the process of multi-criteria decision-making (MCDM) by evaluating and assessing alternative options based on a variety

Table 11 Overall weightage for each criterion

C1	C2	C3	C4	C5	C6	C7	C8
0.084	0.077	0.041	0.044	0.274	0.357	0.076	0.047

of criteria. It consolidates the different criteria into a single utility value, allowing for effective comparison and ranking of the options. In our study, we have determined the weights for each criterion, which indicate their relative importance or priority, as shown in Table 12. By applying the utility function, the performance of each alternative across the various criteria is transformed into a unified utility value. This facilitates the comparison and ranking of the alternatives based on their overall utility, taking into account the trade-offs and preferences associated with the criteria. The calculation of the multi-criteria utility function, incorporating the weights assigned to all the criteria, can be found in Eq. 23.

$$\begin{aligned}\text{Multi-Criteria Utility Function (U)} = {} & 0.084 * [\text{C1}] + 0.077 * [\text{C2}] + 0.041 * [\text{C3}] + 0.044 * [\text{C4}] \\ & + 0.274 * [\text{C5}] + 0.357 * [\text{C6}] + 0.076 * [\text{C7}] + 0.047 * [\text{C8}]\end{aligned} \tag{23}$$

The final step of score and rank is calculated by ranking the alternatives from the sum of decision matrix multiplication by weights using Eq. 23.

The results of the MCDM analysis, including the scores and ranks achieved by the various system configurations, are presented in Table 13. Among the evaluated hybrid energy systems, system configuration 8 obtained the highest score of 0.87, securing the top rank. This indicates that this particular configuration aligns most closely with the identified criteria and demonstrates strong suitability for addressing the technical, economic, and environmental aspects of the project. Following closely in second place is system Configuration 2, which achieved a score of 0.72. On the other hand, the generator-only configuration (system 1) obtained the lowest score of 0.39, placing it in the seventh position. This configuration relies solely on conventional fossil fuel-based power generation, resulting in limited environmental sustainability and higher costs compared to the other configurations.

Table 12 Normalized pairwise matrix

	C1	C2	C3	C4	C5	C6	C7	C8
C1	0.11	0.09	0.15	0.09	0.06	0.08	0.07	0.19
C2	0.02	0.02	0.01	0.04	0.03	0.01	0.01	0.01
C3	0.02	0.03	0.02	0.07	0.04	0.06	0.11	0.02
C4	0.02	0.01	0.01	0.02	0.03	0.04	0.04	0.02
C5	0.46	0.16	0.15	0.16	0.26	0.15	0.13	0.29
C6	0.02	0.03	0.01	0.01	0.03	0.02	0.04	0.02
C7	0.03	0.03	0.05	0.01	0.04	0.01	0.02	0.01
C8	0.05	0.11	0.13	0.11	0.08	0.10	0.13	0.09

Table 13 Score and ranking of the system through MCDM

System	Score	Rank
System 8	0.87	1
System 2	0.72	2
System 5	0.71	3
System 6	0.61	4
System 7	0.57	5
System 4	0.51	6
System 3	0.47	7
System 1	0.39	8

Table 14 Score and ranking of the system through equal weights

System	Score	Rank
System 8	0.68	1
System 2	0.61	2
System 5	0.60	3
System 6	0.57	4
System 7	0.53	5
System 4	0.51	6
System 3	0.43	7
System 1	0.29	8

The prioritization of criteria offers valuable insights into the performance and suitability of each system configuration in meeting the unique requirements of the project. The top-ranked configurations, such as PV/generator/battery and PV/battery, exhibit significant advantages in terms of technical feasibility, economic viability, and environmental sustainability. It is noteworthy that the MCDM rankings align closely with the rankings obtained from the HOMER Pro software.

To validate the results obtained through the SAW-AHP MCDM approach, an additional analysis was conducted by assigning equal weights (0.125) to all eight criteria and applying the MCDM method. This allowed for a comparison with the results obtained from the SAW-AHP MCDM strategy. The multi-criteria utility function becomes:

$$\begin{aligned}\text{Multi-criteria utility function (U)} = {} & 0.125 * [\text{C1}] + 0.125 * [\text{C2}] + 0.125 * [\text{C3}] + 0.125 * [\text{C4}] \\ & + 0.125 * [\text{C5}] + 0.125 * [\text{C6}] + 0.125 * [\text{C7}] + 0.125 * [\text{C8}]\end{aligned} \tag{24}$$

Upon conducting the analysis of the system configurations, it was observed that the ranking of the configurations remained consistent, indicating the robustness of the prioritization process. However, there was a notable decrease in the overall score for system configuration 8, dropping from 0.871 to 0.68. This decline can be attributed to the equal weightage assigned to all criteria, which failed to adequately consider the varying degrees of importance and trade-offs associated with each criterion (Table 14).

Considering all the results obtained, it can be concluded that system configuration 8 emerges as the most viable, sustainable, and reliable option. This configuration exhibits the lowest net present cost (NPC) and levelized cost of energy (LCOE) among all the systems evaluated. Additionally, system 8 achieves zero greenhouse gas (GHG) emissions and demonstrates the capability to provide a continuous power supply to meet the load demands of the area.

7 Conclusion

Due to the geographical location of Pakistan, renewable energy resources are abundant in the country. Distributed generation is the greatest solution to the country's energy issue, but the intermittent nature of renewables makes it difficult to solely depend on one source. Through the optimization of multiple renewable energy supplies in a single hybrid system, this issue can be solved. In hybrid systems, one source complements the other perfectly to provide continuous reliable power. However, the configuration of the hybrid

source significantly depends on the location due to climate and geological conditions. In this study, a hybrid power source is designed for the rural area of Bankhwar Utrar in Kalam, Pakistan. Bankhwar Utrar was selected due to its poor access to the national grid and access to the high potential of renewable energy sources. In examining the techno-economic facets of rural electrification in Bankhwar Utrar, Kalam, Pakistan, this study took into account energy sources such as PV, wind turbines, diesel generator, and battery storage, crafting 8 distinctive hybrid energy configurations. For a local load of 20 kW, the hybrid system was meticulously designed to meet the intrinsic electrical demands of the rural community. A total of eight different systems were designed in HOMER. Systems 1 to 4 were based on the diesel generator with a single renewable source while systems 5 to 8 were based on only renewable sources.

Central to this research was the comprehensive technical analysis of the hybrid systems through HOMER Pro along with the ranking and selection of the most suitable system for the region through the multi-criteria decision analysis (MCDA) technique. The dual methodology, emphasizing both HOMER Pro and MCDA, provided a robust evaluation platform for the various energy scenarios. Key findings from our analysis include:

- The hybrid system of solar PV, wind turbine, hydro turbine, and battery bank (system 8) underscored the limitations of conventional DG-based generation in terms of economic and environmental prudence.
- The aforementioned configuration was championed with an NPC of $166,173.78 and an LCOE of 0.14$/kWh, aligning seamlessly with the energy requisites of Bankhwar Utrar.
- Unsurprisingly, this hybrid configuration topped the MCDA rankings.
- The rankings remained the same for all three scenarios (HOMER Pro ranking, AHP-SAW ranking, equal weights ranking) indicating the reliability and robustness of the model.
- The hybrid system configuration provides the required system stability and sustainability due to the uninterrupted high penetration of renewable energy penetration.
- In terms of environmental stewardship, the system's GHG emissions were a laudable zero, highlighting the ecological merits of the approach.
- The data reveal that in the hybrid system the hydro accounts for a significant portion of the overall electrical production, contributing 52.9% of the total followed by PV with 24.1% while wind provides 23%.
- The hybrid had a significant feasible value of breakeven grid extension distance (BGED) of 75.75 km, which is considerably lower than the actual distance of 112 km between Bankhwar Utrar and the alternate district grid at Kalam.
- Conversely, traditional configurations, notably the diesel generator system and PV/generator hybrid, surfaced as less optimal, both economically and environmentally.
- The sole diesel generator system and the PV/generator hybrid system had the highest NPC of $425,216 and $397,445 with LCOE of 0.36$/kWh and 0.32$/kWh, while also producing GHG emissions of 86168 kg/year and 72097 kg/year.

While this research was specifically tailored to Bankhwar Utrar, Kalam, Pakistan, it is pivotal to note that employing the same HES in a different locale might yield varied results, given the unique geographical and climatic conditions inherent to each area. Nevertheless, the MCDM methodology designed in this study is versatile enough to assess and prioritize systems across diverse locations. Although there might be constraints in universally generalizing the outcomes, the research provides invaluable insights that can act as a touchstone

for the electrification of rural regions. Through its exploration of Kalam's energy demands, potential resources, and localized challenges, this study crafts a blueprint ready for adaptation to other settings. Such adaptability ensures that renewable energy configurations can be fine-tuned to resonate with distinct regional requirements, bolstering their efficacy.

Supplementary Information The online version contains supplementary material available at https://doi.org/10.1007/s10668-023-04350-2.

Acknowledgements The authors are grateful to the Prince Faisal bin Khalid bin Sultan Research Chair in Renewable Energy Studies and Applications (PFCRE) at Northern Border University for its support and assistance.

Data availability Data will be provided upon reasonable request from authors.

Declarations

Competing interests The authors declare that they have no competing interests with any party.

References

Adil Khan, M., Aziz, M. S., Khan, A., Zeb, K., Uddin, W., & Ishfaq, M. (2019). An optimized off-gird renewable AC/DC microgrid for remote communities of Pakistan. In *2019 International conference on electrical, communication, and computer engineering (ICECCE)* (pp. 1–6). IEEE. https://doi.org/10.1109/ICECCE47252.2019.8940636.

Ahmad, Z., Hafeez, M., & Ahmad, I. (2012). Hydrology of mountainous areas in the upper Indus Basin, Northern Pakistan with the perspective of climate change. *Environmental Monitoring and Assessment, 184*(9), 5255–5274. https://doi.org/10.1007/s10661-011-2337-7

Ahmed, J., Harijan, K., Shaikh, P. H., & Lashari, A. A. (2021). Techno-economic feasibility analysis of an off-grid hybrid renewable energy system for rural electrification. *Journal of Electrical and Electronic Engineering, 9*, 7–15.

Akan, A. E. (2021). Techno-economic analysis of an off-grid hybrid energy system with Homer Pro. *Icontech International Journal, 5*(3), 56–61. https://doi.org/10.46291/ICONTECHvol5iss3pp56-61

Al-Badi, A., Al Wahaibi, A., Ahshan, R., & Malik, A. (2022). Techno-economic feasibility of a solar-wind-fuel cell energy system in Duqm, Oman. *Energies, 15*(15), 5379. https://doi.org/10.3390/en15155379

Ali, F., Ahmar, M., Jiang, Y., & AlAhmad, M. (2021a). A techno-economic assessment of hybrid energy systems in rural Pakistan. *Energy, 215*, 119103. https://doi.org/10.1016/j.energy.2020.119103

Ali, M., Wazir, R., Imran, K., Ullah, K., Janjua, A. K., Ulasyar, A., Khattak, A., & Guerrero, J. M. (2021b). Techno-economic assessment and sustainability impact of hybrid energy systems in Gilgit-Baltistan, Pakistan. *Energy Reports, 7*, 2546–2562. https://doi.org/10.1016/j.egyr.2021.04.036

Almasad, A., Pavlak, G., Alquthami, T., & Kumara, S. (2023). Site suitability analysis for implementing solar PV power plants using GIS and fuzzy MCDM based approach. *Solar Energy, 249*, 642–650. https://doi.org/10.1016/j.solener.2022.11.046

Ammari, C., Belatrache, D., Touhami, B., & Makhloufi, S. (2022). Sizing, optimization, control and energy management of hybrid renewable energy system—A review. *Energy and Built Environment, 3*(4), 399–411. https://doi.org/10.1016/j.enbenv.2021.04.002

Awan, M. M., Javed, M. Y., Asghar, A. B., & Ejsmont, K. (2022). Economic integration of renewable and conventional power sources—A case study. *Energies (basel), 15*(6), 2141. https://doi.org/10.3390/en15062141

Bakır, H., Ağbulut, Ü., Gürel, A. E., Yıldız, G., Güvenç, U., Soudagar, M. E., Hoang, A. T., Deepanraj, B., Saini, G., & Afzal, A. (2022). Forecasting of future greenhouse gas emission trajectory for India using energy and economic indexes with various metaheuristic algorithms. *Journal of Cleaner Production, 360*, 131946. https://doi.org/10.1016/j.jclepro.2022.131946

Baseer, M. A., Rehman, S., Meyer, J. P., & Alam, Md. M. (2017). GIS-based site suitability analysis for wind farm development in Saudi Arabia. *Energy, 141*, 1166–1176. https://doi.org/10.1016/j.energy.2017.10.016

Basheer, Y., Waqar, A., Qaisar, S. M., Ahmed, T., Ullah, N., & Alotaibi, S. (2022). Analyzing the prospect of hybrid energy in the cement industry of Pakistan, using HOMER Pro. *Sustainability, 14*(19), 12440. https://doi.org/10.3390/su141912440

Bohra, S. S., Anvari-Moghaddam, A., Blaabjerg, F., & Mohammadi-Ivatloo, B. (2021). Multi-criteria planning of microgrids for rural electrification. *Journal of Smart Environments and Green Computing*. https://doi.org/10.20517/jsegc.2021.06

Chen, Y., et al. (2022). Constraint multi-objective optimal design of hybrid renewable energy system considering load characteristics. *Complex & Intelligent Systems, 8*(2), 803–817. https://doi.org/10.1007/s40747-021-00363-4

Chisale, S. W., & Mangani, P. (2021). Energy audit and feasibility of solar PV energy system: Case of a commercial building. *Journal of Energy, 2021*, 1–9. https://doi.org/10.1155/2021/5544664

Coyle, E. D., & Simmons, R. A. (2014). *Understanding the global energy crisis*. Purdue University Press. https://doi.org/10.26530/OAPEN_469619

Dincer, F. (2011). The analysis on wind energy electricity generation status, potential and policies in the world. *Renewable and Sustainable Energy Reviews, 15*, 5135–5142. https://doi.org/10.1016/j.rser.2011.07.042

Falama, R. Z., Kaoutoing, M. D., Mbakop, F. K., Dumbrava, V., Makloufi, S., Djongyang, N., Salah, C. B., & Doka, S. Y. (2022). A comparative study based on a techno-environmental-economic analysis of some hybrid grid-connected systems operating under electricity blackouts: A case study in Cameroon. *Energy Conversion and Management, 251*, 114935. https://doi.org/10.1016/j.enconman.2021.114935

Hoseinzadeh, S., & Astiaso Garcia, D. (2022). Techno-economic assessment of hybrid energy flexibility systems for islands' decarbonization: A case study in Italy. *Sustainable Energy Technologies and Assessments, 51*, 101929. https://doi.org/10.1016/j.seta.2021.101929

Icaza-Alvarez, D., Jurado, F., Tostado-Véliz, M., & Arevalo, P. (2022). Design to include a wind turbine and socio-techno-economic analysis of an isolated airplane-type organic building based on a photovoltaic/hydrokinetic/battery. *Energy Conversion and Management: X, 14*, 100202. https://doi.org/10.1016/j.ecmx.2022.100202

Iqbal, S., Bilal, A. R., Nurunnabi, M., Iqbal, W., Alfakhri, Y., & Iqbal, N. (2021). It is time to control the worst: Testing COVID-19 outbreak, energy consumption and CO_2 emission. *Environmental Science and Pollution Research, 28*, 19008–19020. https://doi.org/10.1007/s11356-020-11462-z

Islam, Md. R., Akter, H., Howlader, H. O. R., & Senjyu, T. (2022). Optimal sizing and techno-economic analysis of grid-independent hybrid energy system for sustained rural electrification in developing countries: A case study in Bangladesh. *Energies, 15*(17), 6381. https://doi.org/10.3390/en15176381

Jan, S. T., & Noman, M. (2022). Influence of absorption, energy band alignment, electric field, recombination, layer thickness, doping concentration, temperature, reflection and defect densities on $MAGeI_3$ perovskite solar cells with Kesterite HTLs. *Physica Scripta, 97*(12), 125007. https://doi.org/10.1088/1402-4896/ac9e7f

Jan, S. T., & Noman, M. (2023). Analyzing the effect of planar and inverted structure architecture on the properties of $MAGeI_3$ perovskite solar cells. *Energy Technology*. https://doi.org/10.1002/ente.202300564

Kavadias, K. A., & Triantafyllou, P. (2021). Hybrid renewable energy systems' optimization. A review and extended comparison of the most-used software tools. *Energies, 14*(24), 8268. https://doi.org/10.3390/en14248268

Khan, M. I., Khan, I. A., & Chang, Y. C. (2020). An overview of global renewable energy trends and current practices in Pakistan—A perspective of policy implications. *Journal of Renewable and Sustainable Energy*. https://doi.org/10.1063/5.0005906

Kharrich, M., Kamel, S., Alghamdi, A. S., Eid, A., Mosaad, M. I., Akherraz, M., & Abdel-Akher, M. (2021). Optimal design of an isolated hybrid microgrid for enhanced deployment of renewable energy sources in Saudi Arabia. *Sustainability, 13*(9), 4708. https://doi.org/10.3390/su13094708

Kumar, D., & Tewary, T. (2022). Techno-economic assessment and optimization of a standalone residential hybrid energy system for sustainable energy utilization. *International Journal of Energy Research, 46*(8), 10020–10039. https://doi.org/10.1002/er.6389

Lajunen, A. (2014). Energy consumption and cost-benefit analysis of hybrid and electric city buses. *Transportation Research Part c: Emerging Technologies, 38*, 1–15. https://doi.org/10.1016/j.trc.2013.10.008

Mahesh, A., & Sandhu, K. S. (2020). A genetic algorithm based improved optimal sizing strategy for solar-wind-battery hybrid system using energy filter algorithm. *Frontiers in Energy, 14*(1), 139–151. https://doi.org/10.1007/s11708-017-0484-4

Majdi Nasab, N., Kilby, J., & Bakhtiaryfard, L. (2021). Case study of a hybrid wind and tidal turbines system with a microgrid for power supply to a remote off-grid community in New Zealand. *Energies, 14*(12), 3636. https://doi.org/10.3390/en14123636

Nesamalar, J. J. D., Suruthi, S., Raja, S. C., & Tamilarasu, K. (2021). Techno-economic analysis of both on-grid and off-grid hybrid energy system with sensitivity analysis for an educational institution. *Energy Convers Manag, 239*, 114188. https://doi.org/10.1016/j.enconman.2021.114188

Omotoso, H. O., Al-Shaalan, A. M., Farh, H. M. H., & A. A. Al-Shamma'a,. (2022). Techno-economic evaluation of hybrid energy systems using artificial ecosystem-based optimization with demand side management. *Electronics, 11*(2), 204. https://doi.org/10.3390/electronics11020204

Prakash, V. J., & Dhal, P. K. (2021). Techno-economic assessment of a standalone hybrid system using various solar tracking systems for Kalpeni Island, India. *Energies, 14*(24), 8533. https://doi.org/10.3390/en14248533

Rad, M. A. V., Ghasempour, R., Rahdan, P., Mousavi, S., & Arastounia, M. (2020). Techno-economic analysis of a hybrid power system based on the cost-effective hydrogen production method for rural electrification, a case study in Iran. *Energy, 190*, 116421. https://doi.org/10.1016/j.energy.2019.116421

Rafique, M. M., & Rehman, S. (2017). National energy scenario of Pakistan–current status, future alternatives, and institutional infrastructure: An overview. *Renewable and Sustainable Energy Reviews, 69*, 156–167. https://doi.org/10.1016/j.rser.2016.11.057

Rezk, H., Al-Dhaifallah, M., Hassan, Y. B., & Ziedan, H. A. (2020). Optimization and energy management of hybrid photovoltaic-diesel-battery system to pump and desalinate water at Isolated Regions. *IEEE Access, 8*, 102512–102529. https://doi.org/10.1109/ACCESS.2020.2998720

Riayatsyah, T. M. I., Geumpana, T. A., Fattah, I. M. R., Rizal, S., & Mahlia, T. M. I. (2022). Techno-economic analysis and optimisation of campus grid-connected hybrid renewable energy system using HOMER grid. *Sustainability, 14*(13), 7735. https://doi.org/10.3390/su14137735

Rinaldi, F., Moghaddampoor, F., Najafi, B., & Marchesi, R. (2021). Economic feasibility analysis and optimization of hybrid renewable energy systems for rural electrification in Peru. *Clean Technologies and Environmental Policy, 23*(3), 731–748. https://doi.org/10.1007/s10098-020-01906-y

Rosak-Szyrocka, J., Allahham, A., Żywiołek, J., Turi, J. A., & Das, A. (2023). Expectations for renewable energy, and its impacts on quality of life in European Union Countries. *Management Systems in Production Engineering, 31*(2), 128–137. https://doi.org/10.2478/mspe-2023-0015

Sadat, S. A., Faraji, J., Babaei, M., & Ketabi, A. (2020). Techno-economic comparative study of hybrid microgrids in eight climate zones of Iran. *Energy Sci Eng, 8*(9), 3004–3026. https://doi.org/10.1002/ese3.720

Salisu, S. (2019). Techno-economic feasibility analysis of an off-grid hybrid energy system for rural electrification in Nigeria. *International Journal of Renewable Energy Research*. https://doi.org/10.20508/ijrer.v9i1.8873.g7581

Sawle, Y., Gupta, S. C., & Bohre, A. K. (2018). Socio-techno-economic design of hybrid renewable energy system using optimization techniques. *Renewable Energy, 119*, 459–472. https://doi.org/10.1016/j.renene.2017.11.058

Seedahmed, M. M. A., Ramli, M. A. M., Bouchekara, H. R. E. H., Shahriar, M. S., Milyani, A. H., & Rawa, M. (2022). A techno-economic analysis of a hybrid energy system for the electrification of a remote cluster in western Saudi Arabia. *Alexandria Engineering Journal, 61*(7), 5183–5202. https://doi.org/10.1016/j.aej.2021.10.041

Sheikh, M. A. (2009). Renewable energy resource potential in Pakistan. *Renewable and Sustainable Energy Reviews, 13*, 2696–2702. https://doi.org/10.1016/j.rser.2009.06.029

Shezan, S. A., Ishraque, M. F., Muyeen, S. M., Arifuzzaman, S. M., Paul, L. C., Das, S. K., & Sarker, S. K. (2022). Effective dispatch strategies assortment according to the effect of the operation for an islanded hybrid microgrid. *Energy Conversion and Management: X, 14*, 100192. https://doi.org/10.1016/j.ecmx.2022.100192

Silva, B. N., Khan, M., & Han, K. (2020). Futuristic sustainable energy management in smart environments: A review of peak load shaving and demand response strategies, challenges, and opportunities. *Sustainability, 12*(14), 5561. https://doi.org/10.3390/su12145561

Solangi, Y. A., Shah, S. A. A., Zameer, H., Ikram, M., & Saracoglu, B. O. (2019). Assessing the solar PV power project site selection in Pakistan: Based on AHP-fuzzy VIKOR approach. *Environmental Science and Pollution Research, 26*, 30286–30302. https://doi.org/10.1007/s11356-019-06172-0

Sumair, M., Aized, T., Gardezi, S. A. R., Rehman, S. M. S., & ur Rehman, S. U. (2020). Investigation of wind shear coefficients and their effect on annual energy yields along the coastal sites of Pakistan. *Energy Exploration & Exploitation*. https://doi.org/10.1177/0144598720930422

Tariq Jan, S., & Noman, M. (2022). Influence of layer thickness, defect density, doping concentration, interface defects, work function, working temperature and reflecting coating on lead-free perovskite solar cell. *Solar Energy, 237*, 29–43. https://doi.org/10.1016/j.solener.2022.03.069

Tiwari, S., Rosak-Szyrocka, J., & Żywiołek, J. (2022). Internet of things as a sustainable energy management solution at tourism destinations in India. *Energies, 15*(7), 2433. https://doi.org/10.3390/en15072433

Turkdogan, S. (2021). Design and optimization of a solely renewable based hybrid energy system for residential electrical load and fuel cell electric vehicle. *Engineering Science and Technology, an International Journal, 24*(2), 397–404. https://doi.org/10.1016/j.jestch.2020.08.017

Uddin, W., Zeb, K., Haider, A., Khan, B., ul Islam, S., Ishfaq, M., Khan, I., Adil, M., & Kim, H. J. (2019). Current and future prospects of small hydro power in Pakistan: A survey. *Energy Strategy Reviews, 24*, 166–177. https://doi.org/10.1016/j.esr.2019.03.002

Ur Rashid, M., Ullah, I., Mehran, M., Baharom, M. N. R., & Khan, F. (2022). Techno-economic analysis of grid-connected hybrid renewable energy system for remote areas electrification using Homer Pro. *Journal of Electrical Engineering and Technology, 17*(2), 981–997. https://doi.org/10.1007/s42835-021-00984-2

Wahid, S. S. A., Arief, Y. Z., & Mubarakah, N. (2019). Optimization of hybrid renewable energy in Malaysia remote rural area using HOMER software. In *2019 3rd international conference on electrical, telecommunication and computer engineering (ELTICOM)* (pp. 111–115). IEEE. https://doi.org/10.1109/ELTICOM47379.2019.8943925.

Wang, Y., Xu, L., & Solangi, Y. A. (2020). Strategic renewable energy resources selection for Pakistan: Based on SWOT-fuzzy AHP approach. *Sustainable Cities Society, 52*, 101861. https://doi.org/10.1016/j.scs.2019.101861

Zameer, H., & Wang, Y. (2018). Energy production system optimization: Evidence from Pakistan. *Renewable and Sustainable Energy Reviews, 82*, 886–893. https://doi.org/10.1016/j.rser.2017.09.089